FACULTY OF SCIENCE AND TECHNOLOGY

MASTER'S THESIS

STUDY PROGRAMME/SPECIALIZATION: BIOLOGICAL CHEMISTRY	**SPRING SEMESTER, 2018** RESTRICTED ACCESS
WRITER: ALEKSANDRA SZWEDO	**(WRITER'S SIGNATURE)**

FACULTY SUPERVISOR:

ASSOCIATE PROFESSOR HANNE RØLAND HAGLAND

THESIS TITLE:

METABOLIC PHENOTYPE OF LEUKEMIA CELLS AS A DETERMINANT FACTOR FOR THE RESPONSE TO METFORMIN IN DIFFERENT GLUCOSE CONDITIONS

CREDITS (ECTS): 60

KEY WORDS: LEUKEMIA, METFORMIN, MITOCHONDRIA, METABOLISM, METABOLIC REPROGRAMMING	**PAGES:** 72+ APPENDIX: 80 STAVANGER, 15 JUNE 2018

1. ABSTRACT

Cancer cells are known to have highly dysregulated metabolic pathways and altered mitochondria which governs their limited capability of adaptation to nutritional growth conditions. Metabolic flexibility can be reduced by usage of metabolic modulators, like metformin, inhibitor of mitochondrial C–I. Metformin was shown to be associated with reduced risk of cancer development and better overall prognosis. In this study the role of endogenous metabolic phenotype of two leukemia cell lines, HL-60 and Jurkat, was addressed as a determinant factor underlying the response to different glucose growth conditions and metformin treatment. Glucose deprivation was shown to exert anti-proliferative effect in both cell lines, howbeit, stronger in glycolytic Jurkat cell line. Cell line-specific response to metformin was modulated by different glucose concentration. Glucose starvation had a sensitizing effect to the anti-proliferative effect of metformin in both cell lines, however, more pronounced in OXPHOS dependent HL-60. Metabolic stress in HL-60 was reflected by significantly reduced viability and increased reactive oxygen species (ROS) formation. In general, high glucose concentration had a masking effect on the action of metformin, however, it did not protect Jurkat cells against the oxidative stress seen in notably elevated ROS level. To sum up, metabolic reprogramming by glucose concentration alteration was shown to affect the cellular response to mitochondria-targeted drug, metformin and was dictated by the endogenous metabolic capability of the leukemia cell lines. Impairment of mitochondrial respiration appears to be detrimental in both cell lines of different metabolic profiles, hence, underscoring its importance in metabolic flexibility.

2. ACKNOWLEDGEMENTS & CONTRIBUTIONS

At the very beginning I would like to thank everyone that contributed to this work and without whom it could never be completed. The biggest gratitude goes to my supervisor, Associate Professor Hanne Røland Hagland, for granting me the opportunity to become a part of this research. I could never imagine and have never encountered more support regarding all aspects of this work, unconditional understanding, concern and care towards me and every other member of the research team. Thanks to her suggestions, professionalism, thorough academic guidance and open-minded approach, months spent on this study have been filled with challenges, excitement and plenty of questions which never remained unanswered. I am very grateful for this unforgettable experience and all the patience, friendliness and dedication it came with.

I would like to express my gratitude to other members of Hanne research team, as well as academic staff at CORE. Their support and professional advice were invaluable in completion of this work. Especially I would like to thank Julie Nikolaisen for providing me with a training on leukemia cell culture techniques, dedicating her time to guide me through flow cytometry experiments, as well as sharing valuable remarks from her previous work. I would like to express my deepest gratitude to Abdelnour Alhourani for his training on spectrophotometry and flow cytometry, professional advice in the experimental design and a constructive criticism. I would like to thank Preethi Surendran for her advisory support in understanding the procedure and the interpretation of Seahorse assays.

None of the days dedicated to this work would be as wonderful as they were if not the great lab partners I had pleasure to cooperate with, Sam Danby Bailey, Cecilie Lindseth, Ansooya Bokil and Hina Ahmad.

I would like to express a huge gratitude to my family, for their concern and care, constant support and faith I was given despite the long distance between.

Finally, I would like to sincerely thank all my friends and colleagues, for their supportive attitude and understanding.

TABLE OF CONTENTS

3. LIST OF ABBREVIATIONS

NG	No glucose
LG	Low glucose
HG	High glucose
MMP	Mitochondrial membrane potential
ROS	Reactive oxygen species
RT	Room temperature
ATP	Adenosine triphosphate
TCA	Tricarboxylic acid-cycle
GLUT	Glucose transporter
NADH	Nicotinamide adenine dinucleotide
Acetyl-CoA	Acetyl coenzyme A
NADPH	Nicotinamide adenine dinucleotide phosphate
AMP	Adenosine monophosphate
ADP	Adenosine diphosphate
FAD	Flavin adenine dinucleotide
GTP	Guanosine triphosphate
ETC	Electron transport chain
MRC	Mitochondrial respiratory chain
IMM	Inner mitochondrial membrane
IMS	Intermembrane space
OMM	Outer mitochondrial membrane
PMF	Proton motive force
ANT	Adenine nucleotide translocase
VDAC	Voltage-dependent anion channel
UCP	Uncoupling protein
NOX	NADPH oxidase
GSH	Glutathione reductase
GSH/GSSG	Glutathione reduced/oxidized
AKT	Protein kinase B
PI3K	Phosphoinositide 3-kinase
mTOR	Mammalian target of rapamycin
mTORC1	Mammalian target of rapamycin complex 1
mTORC2	Mammalian target of rapamycin complex 2
PTEN	Phosphatase and tensin homolog
PIP2	Phosphatidylinositol 4,5-bisphosphate

PIP3	Phosphatidylinositol 3,4,5-trisphosphate
HIF-1α	Hypoxia-inducible factor 1α
TSC1/2	Tuberous sclerosis complex 1/2
Rheb	Ras homolog enriched in brain
S6K	Ribosomal S6 kinase
4EBP1	4E-binding protein
AMPK	AMP-activated protein kinase
OCT	Organic cation transport protein
PMAT	Plasma monoamine transporter
PKCζ	Protein kinase C ζ
OXPHOS	Oxidative phosphorylation
CaMKK	Calcium/calmodulin-dependent protein kinase
LKB1	Liver kinase B1
ACC	Acetyl-CoA carboxylase
HMG-CoA reductase	3-hydroxy-3-methyl-glutaryl-coenzyme A reductase
p53	Tumor protein 53
VEGF	Vascular endothelial growth factor
REDD1	Regulated in development and DNA damage responses 1
Rag GTP-ase	Recombination-activation gene GTP-ase
TNF-α	Tumor necrosis factor α
IL-6	Interleukin 6
IL-8	Interleukin 8
T1D	Type 1 diabetes
T2D	Type 2 diabetes
IGF-1	Insulin-like growth factor 1
IGF-1R	Insulin-like growth factor 1 receptor
IGFBP	Insulin-like growth factor binding protein
APL	Acute promyeloid leukemia
ALL	Acute lymphoid leukemia
AML	Acute myeloid leukemia
PPP	Pentose phosphate pathway

4. LIST OF TABLES

5. LIST OF FIGURES

6. LITERATURE REVIEW

INTRODUCTION

Cancer has been one of the main focus for the research past decades, reasoned by the fact that it became one of the leading causes of death in many countries [1, 2]. In fact, countries like Denmark, Canada, France, South Korea, Netherlands have been reported cancer as the first mortality cause in 2016 [2]. Moreover, predictions up to date state that the tendency of cancer to take the lead is expected to increase [1]. In 2016 cancers were the second mortality cause worldwide, with 8.93 million deaths, surpassed only by the cardiovascular diseases. In Norway alone, cancers deaths constituted 27.58% of total mortality in comparison to 16.33% observed worldwide [2]. Apart from these data, there are millions of people living with cancer or being cancer survivors [1]. All these taken together accounts for an expanding need for comprehensive understanding of the principal causes, physiology and possible treatment for the disease [1, 2].

What kind of disease the cancer is? This question, although many proposed explanations, remains ambiguously answered, both in terms of the causing factors and origin, preventive actions, potent diagnostic procedures, the character of the disease and the effectual treatment [3–5]. Complex becomes virtually the only right answer, without leaving behind any of the cancer attributes undescribed [1]. Different approaches have been implemented over decades in order to make the cancer comprehension more attainable. For a decent period the cancer research was focused on the theory on the genetic arise of the cancer, supported by nearly 1000 cancer–related genes known commonly dysregulated in the occurrence of the disease in humans [1, 3, 6]. Since 1914, when Theodor Boveri has come out with a proposal of cancer origin from defective chromosomal segregation during mitosis, a substantial attention has been given the genetic–associated cancer rise [3]. Currently, the tumor incidence is generally recognized as the effect of either somatic or germline mutations [4]. The genetic theory has been supported by increasing evidence of mutational accumulation within cancer cells, widely observed chromosomal instability and genetic heterogeneity within a tumor [1, 3]. Apart from the genetic aspect, as early as in 1920, the metabolic approach towards cancer physiology

has been presented by Otto Warburg, in which he pointed out exceptional feature of impaired mitochondrial oxidative phosphorylation in cancer cells, counterbalanced by enhanced glycolysis [1, 3, 4, 7, 8]. Since that time the distinctive metabolic changes in cancer has been under extensive research [6], with a notably intensified focus in the past years, partially due to increased availability and improvement in the metabolomics technology [1]. As the complexity of the disease implies the multidirectional approach to uncover the mechanisms of cancer origin and functionality, insights from both genetic and metabolic findings have led to the conclusion that the reprogrammed metabolism is the phenomenon common for all type of cancers, and thus, it comprises a promising target for the treatment of the disease [1, 3, 4, 6, 7, 9]. In fact, the majority of oncogenes and tumor suppressors have been reported to be linked to the metabolic regulation, which substantially supports the central role of metabolism in cancer functionality [1, 10, 11].

As mitochondria are the organelles responsible for the maintenance of cellular energy balance, they have been of central consideration in terms of cancer origin [6]. Although many aspects of “the cause and the effect” dilemma still retain “the egg and the chicken situation” nature, enough evidence has been collected to regard mitochondria as the pivotal element of cancer research and the promising target for future therapies [6]. This has given an inspiration for the presented thesis, which would hopefully contribute to the future improvement of cancer understanding and more potent treatment as a result. The role of metabolic phenotype as a key factor for adaptation to different growth conditions and responsiveness to a mitochondria targeted drug, metformin, is the main aim of this study. The experimental work is conducted using two leukemia cell lines of distinct metabolic profiles in order to provide a comparative evaluation of the results.

CANCER

Cancers have been classically viewed as a disease that is characterized by an aberrant growth of the cells with the eventual metastasis to other locations within an organism [5]. Morbidity and mortality in cancer is mainly due to metastasis [4].The reasons behind cancer occurrence are still a topic of controversy. In terms of genetic, both hereditary/germline and somatic mutations are considered to be originators of the disease, with germline mutations constituting only 5-7% of all cancers [4]. Also, it is well

established that prolonged lifespan and lifestyle/environmental factors (e.g. carcinogenic substances, radiation, smoking, alcohol, obesity) contribute to cancer arise, the first by the gradual buildup of genetic and structural defects in the cell and, the second, by mutagenic character [4, 10]. Other factors, as viral infections, have also been recognized to contribute to cancer development [4]. In fact, most of the tumorigenic factors could be collectively viewed as positive feedback phenomenon, which, together with unspecified primary cause, could explain the difficulty in targeting the disease, reflected by persistently high cancer mortality [3] and lack of treatment efficiency [6].

In 2000, Hanahan and Weinberg proposed six physiological alterations that may be crucial for abnormal cell behavior [12]. These are known as the “hallmarks of cancer” and involve: 1) self-sufficiency in growth signals, 2) insensitivity to growth inhibitory, 3) evasion of programmed cell death, 4) limitless replicative potential, 5) sustained vascularity and 6) tissue invasion and metastasis [4, 5, 12]. A rational explanation for the cells to manifest the suggested hallmarks is the genome instability which enhances the mutation occurrence. However, this view is debated as unlikely to be the only cause underlying the malignant shift in the cell, since the accumulation of aberrant mutations is required to be higher than what is currently observed [4]. Hence, other factors must be involved in the malignant phenotype transition.

GLUCOSE METABOLISM

To maintain functionality, all cells need to keep an energetic homeostasis (of -56kJ/mol) by regulating the level of ATP, the universal metabolic currency. Even a slight change in the cellular ATP level affects the cell physiology: ATP deficiency eventually triggers cell death by apoptosis [13] while ATP surplus affects membrane pumps, respiration and viability [6]. Primarily to fatty acids and amino acids, glucose is the basic substrate to generate ATP, with the maximal energy yield of 36 ATP per molecule achieved through glycolysis, TCA cycle and oxidative phosphorylation (**Table 1**) [6].

Glycolysis. Glycolysis is an oxygen-independent, initial glucose metabolism pathway. It is thought to evolve in organisms adapted to non-oxygen containing atmosphere and thus constitutes the primordial energy generating pathway [5]. The process of glycolysis occurs in the cytoplasm and involves 10 enzymes subsequently degrading glucose into pyruvate

[5, 14]. Once glucose enters the cell through glucose transporters (GLUT), it becomes irreversibly phosphorylated by hexokinase [15]. Two steps in the initial phase of glycolysis require energy expenditure of 1 ATP each [5]. The net balance/yield/output of complete glycolytic conversion of one molecule of glucose is 2 molecules of pyruvate (3-carbon compound), 2 ATP and 2 NADH molecules [15]. Depending on oxygen availability and cellular needs, pyruvate can be further anaerobically converted into lactate in the cytosol or converted into acetyl-CoA to fuel further metabolic pathways in mitochondria [5].

TCA cycle. Upon the conversion into acetyl-CoA by pyruvate dehydrogenase and transportation into the mitochondrial matrix, pyruvate generated in the last step of glycolysis can be incorporated into TCA cycle. Acetyl-CoA combines with oxaloacetate to continue TCA cycle, which is a series of eight enzymatic reactions leading to oxidation of intermediates into carbon dioxide (CO_2), with a parallel reduction of NAD^+ and FAD into NADH and $FADH_2$, respectively[15]. The net gain of full TCA cycle per one molecule of acetyl-CoA is 1 GTP (ATP) molecule, 3 NADH and 1 FADH2 of reduced coenzymes (electron carriers) [15].

Apart from glucose, other substrates like fatty acids and amino acids can also fuel the TCA cycle. Upon β-oxidation, acetyl-CoA generated from fatty acids can directly enter the TCA cycle. Amino acids can be converted to pyruvate, acetyl-CoA or intermediates of TCA cycle and thus enter the pathway in multiple ways. NADH and FADH2 are important products of TCA cycle which can then serve as electron donors in the process of oxidative phosphorylation coupled with electron transport chain (ETC) [16].

Oxidative phosphorylation (OXPHOS): mitochondrial respiratory chain/electron transport chain. The process of oxidative phosphorylation combines mitochondrial respiratory chain (MRC) and ATP synthesis, involving in total five protein complexes localized in the inner mitochondrial membrane (IMM) [17]. The first four complexes of MRC, (I-IV), also termed as the electron transport chain (ETC) [16], are involved in proton transport from the mitochondrial matrix into the intermembrane space (IMS). Active transport of H^+ via IMM against the gradient is supplied with energy from the electrons donated to C–I and C–II. C–I (NADH: ubiquinone oxidoreductase), a transmembrane protein complex, accepts electrons from the reduced form of NADH, utilizing the high

energy of electrons to pump out protons through IMM. Electrons from the oxidation of TCA cycle intermediate, succinate, into fumarate are donated to C–II (succinate: ubiquinone oxidoreductase). Electrons from both C–I and C–II are translocated to ubiquinone (coenzyme Q, CoQ), reducing it to ubiquinol (QH_2), and then shuttled to C–III (ubiquinol: cytochrome c oxidoreductase). Similarly, energy of the electrons flowing through C-III is used to transfer protons across IMM. From C–III electrons are translocated to C-IV (cytochrome c oxidase) by cytochrome c (Cyt C), where their energy potential is utilized for both proton transfer and reduction of O_2, final electron acceptor, to H_2O in the matrix [17].

ATP synthesis. Proton motive force (PMF), termed also as mitochondrial membrane potential (MMP), created through the ETC, is a sum of transmembrane proton concentration (pH) and electric potential [16]. It constitutes a motive force of high potential, which can be utilized to power the ATP synthase (complex V) to fuel the ADP phosphorylation. ATP synthase is a transmembrane protein complex that allows proton flow from IMS back to mitochondrial matrix and couples it with ATP synthesis [17]. ATP is generated in the mitochondrial matrix and it can be utilized within mitochondria or translocated outside via adenine nucleotide translocate (ANT) and voltage-dependent anion channel (VDAC) across IMM and OMM, accordingly [14]. An important function of ATP synthase is the ability to hydrolyze ATP, which constitutes an additional mechanism for energetic balance within the cell [6].

The efficiency of OXPHOS and functionality of protein complexes depends highly on the IMM integrity and structural content [6]. IMM was shown to require specific lipid content in order to maintain the impermeability, essential for proton leakage prevention. Cardiolipin, 1,3-diphosphatidyl-sn-glycerol, a phospholipid present almost exclusively in IMM, is directly associated with the stabilization of ETC super complexes and the functionality of OXPHOS complexes [3, 4, 6]. There is evidence that cardiolipin and ETC protein complexes evolved in close association, which emphasizes the importance of proper lipid content of IMM for OXPHOS maintenance [4]. Apart from changes in IMM lipid content, the presence of uncoupling proteins (UCPs) is also linked to the proton leakage leading to decrease in membrane potential and increased uncoupling of respiration from phosphorylation [6].

The flow of the electrons through ETC is prompt to lead to their leakage, which in turn facilitates ROS formation. C–I, C–III and, to a lesser extent, C–II, are the sites at the highest risk of ROS production to occur [17].

Table 1 ATP yield through glucose metabolism. Values given per 1 molecule of glucose

PROCESS	TYPE	LOCATION	Net ATP yield
Glycolysis	Substrate-level phosphorylation	Cytoplasm	2 ATP
TCA cycle		Mitochondrial matrix	2 ATP
OXPHOS	Oxidative phosphorylation	Mitochondrial matrix/IMM	32 ATP
		TOTAL	36 ATP

FUNCTION OF MITOCHONDRIA IN CELLULAR METABOLISM

Origins of mitochondrial science. In line with endosymbiotic theory, mitochondria originated through the endosymbiotic interdependence of an α-proteobacteria incorporated into eukaryotic cell host [18]. In the historical point of view, mitochondria were first described as granular cellular elements, later thought to be associated with basic activity of the cell in 1890s. However, structures representing mitochondria were observed earlier in 1840s. The term ‘mitochondrion’ originating from ‘mitos’ (gr. thread) and ‘chondros’ (gr. granule) was introduced in 1898 by Benda, replacing the ‘bioblast’ term used earlier by Altmann [14, 19].

Mitochondrial structure. Structure and number of mitochondria differs depending on the type of tissue. The standard dimensions of the organelle are 1-2 μm length and 0.5-1 μm width. Mitochondria have two lipid-bilayer membranes, outer mitochondrial membrane (OMM) enclosing the organelle, and IMM folded into multiple cristae. Cristae significantly increase the surface of the inner membrane, where protein complexes of OHPHOS are located, which enhances the oxidative phosphorylation capacity [6, 14]. Two sets of membranes divide mitochondrion into four compartments: OMM and IMM, IMS, which encompasses the space between OMM and IMM, and mitochondrial matrix, inner space

of the organelle restricted by IMM. Compartmentalization of mitochondria allows for conducting simultaneously processes that require differential conditions to occur [14].

Mitochondria possess the ability to fragment and fuse with each other, which allows for dynamic change of mitochondrial content within the cell [14].

Mitochondrial genome. Mitochondria possess their own DNA, termed mitochondrial DNA (mtDNA). In comparison to the total DNA content within the cell, mtDNA constitutes only less than 1%. mtDNA is only inherited maternally [20]. Mammalian mtDNA is characterized by lack of both introns and histones, which are associated with higher risk of mtDNA damage. It is thought that mutation occurrence in nuclear DNA (nDNA) is around tenfold lower than in mtDNA [14]. In healthy cells, mtDNA sequences within all mitochondria are considered to be homoplasmic (identical). Somatic mutations may lead to heteroplasmy, which after surpassing a certain level, eventually cause mitochondrial abnormalities [14]. Heteroplasmy threshold varies among tissues and is relatively low in those of high oxidative metabolism demand [20].

Reactive oxygen species (ROS). ROS are unstable, highly reactive by-products of oxygen-dependent metabolism [21] and include superoxide anion ($O_2^{\bullet -}$), hydrogen peroxide (H_2O_2) and hydroxyl radicals ($OH^{\bullet -}$), the last being the most reactive [22]. Mitochondria have the largest contribution to cellular ROS, which is directly linked to the OXPHOS metabolism. It is approximated that 1-3% of electrons passing through ETC undergo leakage, especially on C–I, C–III and cyt C [20]. Apart from mitochondria, ROS formation is linked to the activity of cytochrome P450 in ER, lipoxygenases, cyclooxygenases, xanthine oxidase (XO) and cellular NADPH oxidases (NOX) [20]. ROS can be neutralized by enzymes present in the cytosol or mitochondria. Superoxide anion generated mostly by C–I and C–III is reduced into H_2O_2 by Mn superoxide dismutase (MnSOD; SOD2) in the matrix or Cu/Zn superoxide dismutase (Cn/ZNSOD; SOD1) in IMS and cytosol, respectively [22]. Further neutralization of H_2O_2 is conducted by glutathione peroxidase (GPx), using electrons donated by reduced form of glutathione (GSH). Glutathione reductase (GSR) regenerates GSH from its oxidized form (GSSG), simultaneously oxidizing NADPH to NADP+ [22]. However, H_2O_2, when generated in excessive amounts, can undergo metal–catalyzed reaction yielding highly reactive, $OH^{\bullet -}$

radicals [22]. Cellular iron homeostasis has a preventive role against hydroxyl radical formation [21].

Enhanced ROS formation has been shown to occur in isolated mitochondria under two conditions: 1) in presence of high NADH/NAD+ matrix ratio, and 2) when highly reduced CoQ amount is present in mitochondria with high PMF and no ATP synthesis occurring. Normally functioning mitochondria, utilizing PMF for ATP synthesis or other processes, produce ROS, however, in comparably insignificant amounts [22, 23].

Role of ROS. ROS have been long associated with the oxidative stress of cells, which is linked to ROS instability and reactivity, driving the ROS to readily modify cellular components: proteins, lipids and nucleic acids [21]. Out of the previously mentioned ROS, hydroxyl radical has the highest potential regarding cellular damage, which arises from its indiscriminate oxidation of molecules within the cell [21]. ROS are considered as the main source of human DNA alternation. The total contribution of ROS to DNA damage are estimated as 10,000 nucleotides in DNA per day in one cell, which constitutes around 20% of total modifications arising from cellular metabolism alone [24].

Also, ROS are thought to be an important part of cellular signaling. It has been shown that there are specific proteins, superoxide-inactivated, which initiate pathways leading to cell death or adaptation to enhanced superoxide level in the cell [21]. Therefore, oxidative stress may no longer be viewed as a damaging process, but also an inherent part of stress responsive signaling [21], referred to as redox signaling. Since ROS are characterized by relatively short half-time and instability, redox signaling requires proximity between the source of ROS signaling molecules and ROS-dependent receptors. Dynamic movements of mitochondria are recognized as aimed to facilitate activation of redox signaling pathways [21].

ROS shuttle between cancer cells and cancer associated fibroblasts (CAFs) has been shown to play an important role in reverse Warburg effect and metabolic reprogramming of cells within tumor microenvironment [8].

ALTERATIONS IN CANCER METABOLISM

As mentioned before, Warburg observed that cancer cells differ in terms of glucose metabolism, using up to 200 times more glucose in comparison to normal cells [1], and turning it into lactate, regardless of non-hypoxic conditions [5]. According to Warburg theory, the initiation of tumorigenesis is driven by insufficient respiration, which in turn causes gradually intensified glycolysis and aerobic fermentation of lactate, in the end leading to irreversible impairment of energy generation by oxidative respiration [3].

This view can be supported by enhanced expression of glycolysis – related genes in most of the cancers [4, 5]. Originally, the insufficient respiration was believed to be an effect of mitochondrial damage [11]. In fact, even though the abnormalities in tumor mitochondria are well documented across the majority of cancers, functional organelles are present and active in most of the tumors, at least in the initial phase of tumor development [5, 11]. Therefore, the pro-glycolytic behavior of the cells to become tumorigenic remains unclear, with growing evidence of epigenetic regulation having a crucial role in cancer arise [10].

Evaluation of different types of cancer revealed that despite a large amount of genetic mutations detected collectively, certain tumors are rarely assigned a specific type of gene abnormality [4]. Heterogeneity is observed not only between different types of tumors, but often also between different cells within a tumor. This creates a challenge for genetic-based diagnosis of cancer, reduces the potential of gene therapies and partly explains their failure [3].

Notably, the shift in energy metabolism has been documented for nearly all types of cancer, regardless of its etiology and tissue of origin [5]. As different carcinogenetic factors as viral infection and the chemical compound may evoke similar mitochondrial and enzymatic dysfunctionality [4]. In terms of metabolism, cancer seems to represent more homogeneous disease. Metabolic reprogramming and glycolysis-oriented phenotype are currently considered as one more hallmark of cancer [8, 11].

Loss of metabolic flexibility in cancer cells. With all the mutations accumulated within tumor cells, the metabolic flexibility is thought to be significantly reduced in comparison to normal cells. Even though tumors outgrow the normal tissues, this phenomenon is mostly observed when the fermentable substrates are unlimited. In other words, cancer cells

develop adaptations to utilize the abundantly present substrates (by following the evolution principles). However, metabolic reprogramming leading to higher glucose turnover may lead to the loss of flexibility under metabolic stress and increase in susceptibility to nutrient depletion [3, 4, 6]. In fact, low calorie and ketogenic diets have been proposed as an effectual adjuvant approach in cancer treatment due to reduction of easily available nutrients for cancer growth [3].

MOST DYSREGULATED PATHWAYS

PI3K/Akt/mTOR pathway. Normal cells within an organism constitute one cooperative entity with tightly regulated interrelations to maintain homeostasis in a response to both regular and abnormal conditions in environment and within single cells [25]. However, cancer cells undergo reprogramming in order to sustain their mutations-driven highly proliferative and invasive behavior. One of the most dysregulated pathway observed in most of cancers is PI3K/Akt signaling [26]. Akt expression was shown to be elevated in cancer cells [6]. PI3K/Akt/mTOR pathway was shown to be amplified in 60-80% AML patients [27]. Akt, known also as PKB (protein kinase B), is a serine/threonine kinase, controlling numerous pathways involved in energy metabolism, proliferation and apoptosis inhibition [6]. There are three different isoforms of Akt: Akt 1, Akt 2, extensively expressed in hematopoietic stem cells, and Akt 3 [28]. Akt is activated by PI3K, triggered by growth factors, including insulin [29]. Akt stimulates GLUT1 and GLUT4 membrane translocation and phosphorylates several enzymes involved in glycolysis, enhancing the glucose uptake and metabolism [30]. Akt signaling is suppressed by PTEN, which hydrolyzes PIP-3 to PIP-2, inhibiting the downstream signaling of PIP-3 [5]. Mutations in PTEN are linked to dysregulated Akt/mTOR pathway. Moreover, PTEN-inactivating mutations, as well as PI3K-mediated mTOR activation were both shown to affect HIF-1α activation [5]. In general, activated PI3K/Akt pathway determines glucose-dependent, glycolytic profile [5].

mTOR. mTOR, a serine/threonine protein kinase, is an important regulator of cell survival and growth, present in the cell in two functionally distinct complexes, mTORC1 and mTORC2. mTORC1, a TSC1/2/Rheb-regulated downstream target of Akt signaling, exerts stimulatory effect on protein synthesis via its effectors S6K and 4EBP1, whereas

mTORC2, upstream in regard/relation to Akt, can fully activate it by S473 phosphorylation [28].

TSC1/2 constitutes a significant node in negative regulation of mTORC1 by two distinct kinases, AMPK and Akt. AMPK-driven phosphorylation activates TSC1/2, implying mTORC1 inhibition, whereas TSC1/2 phosphorylation by Akt silences its mTORC1 inhibiting function, consequently activating the kinase [28]. Apart from TSC1/2-mediated mTORC1 inhibition, several other pathways have been shown for AMPK-stimulated downregulatory effect on mTORC1 [26, 31].

METFORMIN MODE OF ACTION

History of metformin. Medical use of the plant, *Galega officinalis*, dates back to medieval times. Galegine, an active ingredient was utilized originally for the synthesis of biguanides, compounds of antihyperglycemic agents. One of them, metformin, was originally introduced in 1957 [31], and reached the state of the most widely prescribed treatment in type 2 diabetes (T2D) [26, 32]. Metformin is well tolerated, has a positive impact on endothelium and serum lipid profile, which together with low side-effect incidents of lactate acidosis (3.3 cases per 100,000 [33]) makes it a successful drug. Moreover, in 2005 the first observation of reduced risk of cancer in T2D patients treated with metformin was noted, lately confirmed by numerous epidemiological studies [31]. This notable effect brought attention to metformin as a potential agent in cancer prevention and treatment and, has driven extensive studies on possible mechanisms involved in the action of the drug.

Physicochemical properties. Metformin is a basic compound with pKa values of 2.8 and 11.5, and thus in physiological pH range exists in a cationic form (>99.9%). The hydrophilic character of metformin (logP = -1.43) makes passive diffusion of via cellular membranes unlikely, therefore uptake of the drug is associated with organic cation transporters OCTs) [33].

Pharmacokinetics in oral administration. Upon single-dose oral administration, the drug takes approximately 3 h to achieve its peak plasma concentration of 1.0 – 1.6 mg/L after 0.5 g dose. Absorption of metformin in the gastrointestinal track is incomplete, with

the bioavailability reported to reach 55 ± 16%. Uptake of metformin from small intestines into enterocytes occurs mainly via plasma membrane monoamine transporter (PMAT). OCT1 and OCT3 drive the uptake both in liver and peripheral tissues, where metformin is delivered in plasma protein-unbound form. Varying OCT1 expression in hepatic cells may be a pivotal factor in overall response to metformin treatment [33, 34], as the exposure of liver to metformin is high due to portal circulation from small intestine [35]. Metformin in its unchanged form is excreted in urine [33, 34].

Metformin effect. Beneficial effect of metformin in T2D is linked mostly to hepatic gluconeogenesis inhibition and increased glucose uptake and turnover in peripheral tissues via an increased sensitivity to insulin. Metformin exerts reducing effect on insulin secretion by β-pancreatic cells, therefore it decreases plasma insulin level [26]. Use of metformin, unlike other anti-diabetic drugs, is not related to weight gain, furthermore, slight weight loss was shown to be associated with metformin based therapy [35]. Most of these effects are attributed to AMPK, a kinase of executive response to high AMP/ATP ratio in the cell [36].

Overall metformin impact on metabolism is traditionally divided into indirect (insulin-dependent) and direct (insulin-independent) pathways, which act complementary to exert the ultimate effect of the drug [37]. Regarding cancer cells, the overall effect of metformin is highly determined by their transformation stage and metabolic profile [26, 32].

DIRECT MODE OF METFORMIN ACTION

Complex I inhibition. It is suggested that metformin regulatory impact on overall metabolism is a downstream effect of C–I inhibition [37]. Due to its cationic form, drug accumulates in the negatively charged mitochondrial matrix and directly inhibits C–I [35], increasing the contribution of uncoupled respiration. Despite yet unknown inhibitory mechanism, limitary C–I activity was shown both *in vivo* and in isolated C-I [35]. Inefficient mitochondrial ATP yield increases cellular AMP/ATP ratio, consequently activating AMPK. Furthermore, reactive nitrogen species formation as a consequence of MRC inhibition was suggested to activate LKB1, upstream AMPK activator, via PKCζ [31].

AMPK activation. Enhanced AMP/ATP ratio leads to cellular metabolism shift from anabolic to catabolic exerted by activated AMPK. Phosphorylation of AMPK on Thr172 residue is a requirement for its activation and is conducted by LKB1 and calcium/calmodulin-dependent protein kinase (CaMKK). Expression of gluconeogenesis associated genes in the liver is further suppressed by AMPK–mediated phosphorylation of transcriptional factor TorC2 (transducer of regulated CREB protein2) [36]. By exerting a direct downregulatory effect on enzymes, ACC and HMG-CoA reductase, AMPK impairs fatty acid and cholesterol biosynthesis, respectively, processes involved in malignant tumor transformation [31]. p53 is another downstream target of activated AMPK, stimulating compensatory β-oxidation, amino acid catabolism and autophagy in energy deficient cells. It was shown that metformin treatment of p53 depleted cancer cells, consequently unable to execute metabolic adaptation, led to apoptosis [26].

mTOR inhibition. mTOR is an important effector of PI3K/Akt pathway, regulating the cellular growth and proliferation mainly via protein synthesis control in a response to the growth factors and energy balance of the cell. Moreover, mTOR stimulates HIF-1α and VEGF, contributing to angiogenesis, crucial for tumor progression [37]. Metformin induced inhibition of mTOR, an important PI3K/Akt effector, reduces activity of its effectors, 4E-BP1 (4E-binding protein) and S6K (ribosomal S6 kinases) [26]. AMPK-dependent mTOR inhibition is executed by several pathways: p53/REDD1, TSC1/2/Rheb and AMPK/Raptor [31]. Apart from these, AMPK-independent Rag GTPase pathway was suggested [38].

Anti-inflammatory effect. AMPK inhibitory downregulation of TNF-α, IL-6, IL-8 and VEGF makes them subjected to metformin action, and thus constitutes anti-inflammatory anti-proliferative effect of the drug [36].

TCA cycle. Metformin, by uncoupling the mitochondrial respiration, has a negative effect on the accumulation of TCA cycle intermediates [26], which can be otherwise utilized as precursors for biosynthesis of fatty acids and amino acids, important for cancer cell growth [32]. The load of TCA cycle substrates into the mitochondria is further decreased by metformin-driven pyruvate dehydrogenase inhibition, enzyme converting pyruvate into acetyl-CoA [39]. Changes of metabolic intermediates levels consequently affect the

epigenetic DNA modifications requiring them as acetyl, phosphate and methyl donors for acetylation, phosphorylation and methylation of histones, respectively [26].

INDIRECT MODE OF METFORMIN ACTION

In human metabolism, insulin, commonly used as a drug in both T1D and T2D, plays a role of a growth factor and thus exhibits a mitogenic effect. In fact, a few types of cancers have been reported an increased plasma insulin levels [37]. IGF-1, growth factor of higher mitogenic nature, upon binding with IGF-IR on cell surface promotes tumorigenesis by Ras/Raf/MER/ERK and PI3K/PDK1/Akt/mTOR cascades. Moreover, IGF-1 halts PTEN, the PI3K/PDK1/Akt/mTOR inhibitor [26]. Metformin, by lowering the blood glucose, decreases the insulin level, which in turn promotes binding of IGF-1 to IGF-binding protein (IGFBP), reducing its unbound, potentially mitogenic form in the blood plasma. Moreover, AMPK-dependent phosphorylation of insulin receptor substrate (IRS-1) negatively regulates the PI3K/PDK1/Akt/mTOR pathway [37].

LEUKEMIA

Early history of leukemia. Leukemia is a cancer of specific types of blood cells. Leukemia is distinctive from majority of cancers which form solid tumors. In contrary, leukemia arises from blood precursor cells and exists mainly in human circulatory system [40], which was the major reason for impeded diagnosis and recognition of the disease as cancer. Early cases regarding patients with both abnormal white blood cells in blood material and unnaturally enlarged spleens were described in 1820s [40, 41]. For the first time, the term ‘leukämie’ was introduced by Rudolf Virchow in 1847, a year after leukemia has been diagnosed in a patient during life for the first time in 1846. A breakthrough in leukemia history occurred in 1869, when Ernst Neumann linked the disease origin with bone marrow [41, 42].

Leukemia is closely related to the process of hemopoiesis, the blood cells formation from their precursors present in bone marrow. Bone marrow is where most of pluripotent stem cells are located, which upon division give rise to either lymphoid or myeloid stem cells [40]. Then, after differentiation, progenitor lymphoid and myeloid stem cells mature into more specialized lineages of blood cells. Leukemia arises when hemopoiesis is disrupted

at certain stage and undifferentiated progenitor cells undergo multiplication. Recently, the importance of leukemic stem cells (LSCs) was emphasized, due to their potential role in leukemia relapse and possible protective interrelations with bone marrow microenvironment, resembling classical solid tumors [43].

Genetic factors causing leukemia. It is estimated that only around 5% of leukemia cases are caused by inherited gene defects [42]. Furthermore, few inherited genetic disorders are shown to increase the risk of developing leukemia [40].

External factors causing leukemia. Risk factors associated with leukemia occurrence involve i.a. high-energy radiation exposure, certain chemicals, pesticides and some viral infections [40]. There is no evidence on dietary habits affecting the risk of leukemia development [42].

Types of leukemia. Leukemia comprises many different types, which are distinguished on the basis of type and maturity of hematopoietic cell lineage it originates from as well as the progression rate of the disease. Acute leukemias develop from immature, undifferentiated hematopoietic cells, and are characterized by rapid clinical evolution. On contrary, chronic leukemias have longer clinical evolution due to more mature cells of origin. Two early distinct hematopoietic progenitor lineages are lymphoid and myeloid [43]. Therefore, four major leukemia types involve: 1) acute lymphocytic leukemia (ALL), 2) chronic lymphocytic leukemia (CLL), 3) acute myelogenous leukemia (AML) and 4) chronic myelogenous leukemia [40]. In this thesis, two cell lines, Jurkat and HL-60 are used, representing ALL and APL (acute promyelocytic leukemia), subtype of AML, respectively [45].

7. AIMS OF STUDY

BACKGROUND/RATIONALE

The overall aim of this study was to evaluate the response of two leukemia cell lines to the metabolic drug metformin in different glucose growth conditions.

OBJECTIVES

The study was performed to determine the response to metformin of two leukemia cell lines, HL-60 and Jurkat, upon metabolic reprogramming in different glucose growth conditions. The evaluation involved the impact on proliferation, viability, MMP, mitochondrial content and cellular ROS levels. Final interpretation was supported by metabolic phenotypes of two cell lines assessed in the study.

SPECIFIC AIMS

- Determination of metabolic phenotype of two leukemia cell lines;
- Identification of the relationship between metabolic phenotype of two leukemia cell lines and their ability to grow under different glucose conditions;
- Evaluation of metabolic phenotype and glucose growth conditions impact on the response to treatment with the metabolic drug, metformin;
- Determination of metabolic phenotype, glucose growth conditions and metformin treatment influence on mitochondrial membrane potential and reactive oxygen species formation change.

8. MATERIALS AND METHODS

LEUKEMIA CELL LINES & CULTURING CONDITIONS

Two leukemia cell lines, HL-60 and Jurkat, used in this thesis were a gift from the research group of Professor Karl J. Tronstad, University of Bergen. Passage numbers at the start of the research were unknown. Experiments were conducted using the cells of passage number below 15 from the moment of starting the culture. Originally, HL-60 and Jurkat cell lines were isolated from peripheral blood of patients with APL and T-cell ALL, respectively [44]. Moreover, according to available publications, two cell lines exhibit distinct metabolic phenotypes [45], which was also observed in unpublished study from University of Bergen by Hanne R. Hagland, the supervisor of this research, and Julie Nikolaisen.

Both cell lines were grown in suspension of density 400 000 – 600 000 cells/ml in 75 cm^2 flasks. Experiments were conducted with different starting cell densities, as described in **MATERIALS AND METHODS** section. Culturing media was RPMI 1640 medium of 2 g/L glucose and 300 mg/L glutamine, supplemented with 10% fetal bovine serum, 100 U/ml penicillin and 100 µg/ml streptomycin. Cells were kept in 5% CO_2 humidified incubator (SANYO Electric Co., Lts., Japan) at 37°C when routine culturing and during the experimental work, unless indicated differently. All the experiments were conducted using both cell lines, unless stated otherwise.

MATERIALS AND INSTRUMENTS USED IN THE STUDY

The list of reagents (**Appendix: Table 9**) and list of instruments and software (**Appendix: Table 10**) used in this study are enclosed in the **APPENDIX** section.

GLUCOSE GROWTH CONDITIONS

To study the response of two leukemia cell lines of distinct metabolic profiles, three different glucose growth conditions were used in the experiments, as described in **Table 2**, unless stated differently.

Table 2 Glucose growth conditions used in the experiments

Condition/ concentration	DESCRIPTION
HG **2 g/L** **11.1 mmol/L**	HG condition corresponds to the glucose concentration in the standard culture of leukemia cells. HG shows the response of the cells to the unlimited/abundant glucose. HG conditions do not refer to normal physiological conditions found within human blood system in healthy individuals. Occasionally, HG concentration is observed as postprandial glycemia in diabetic people.
LG **1 g/L** **5.5 mmol/L**	LG condition represent the physiological glucose concentration referred to as fasting blood sugar. LG condition is used to study the response of the cells in physiological conditions, most likely to occur in human body.
NG **0 g/L** **0 mmol/L**	NG condition illustrates the metabolic response to glucose deprivation, testing the metabolic adaptation and flexibility of the cells, driving the cells to utilize OXPHOS [46]. Moreover, it uncovers the role of glucose on cellular metabolism, when compared with LG and HG, and is of additional value when determining the metabolic phenotype of different cell lines. NG conditions illustrate the locations in the human body depleted for glucose which may occur in tissue distant from blood vessels, like the compartments inside the solid tumor. Therefore, while NG conditions used in the experiments relate only to glucose inaccessibility, in vivo, they may be directly linked to the depletion of other nutrients, as well as oxygen, caused by impaired supply means. Thus, NG conditions used in combination with a drug in the experiments may not reflect the real mode of action in a living organism due to lower achievable drug concentration.

METFORMIN AS ENERGY METABOLISM MODULATOR

This research was aimed at metformin as a modulator of energy metabolism, more specifically, its direct mode of action (accumulation in mitochondrial matrix, inhibition of C-I and mitochondrial depolarization).

The starting range concentration of metformin was chosen to be within range of 0.1 mM to 5.0 mM, reported in many research of this kind [47, 48]. This range exceeds the physiological concentration achievable in human blood stream. Selection of these concentration values was supported by the purpose of the research, which is to study the metformin impact on the metabolism of leukemia cells rather than the clinical importance in terms of leukemia treatment *per se*, unless proved otherwise.

Metformin concentrations used in the first proliferation assay, Alamar Blue, were 0.1 mM, 0.5 mM, 1.0 mM, 3.0 mM, 5.0 mM. Based on the observed response, the second proliferation assay, BrdU, was performed with 0.1 mM, 1.0 mM and 3.0 mM, accordingly. Results obtained from previously mentioned assays have led to the final selection of 0.1 mM and 3 mM for the further experiments.

EXPERIMENTAL GROUPS LAYOUT

As mentioned above, the variable experimental conditions were used in the study. The table below (**Table 3**) presents settings applied throughout the tests.

Table 3 Experimental design outlook. Table includes the type of assay, incubation time of the samples, glucose growth condition and metformin concentrations used, as well as cell lines involved.

<table>
<tr><th rowspan="2">CELL LINES</th><th rowspan="2">ASSAY NAME & DURATION TIME</th><th colspan="6">GLUCOSE GROWTH CONDITIONS & METFORMIN CONCENTRATION</th></tr>
<tr><th colspan="2">NG</th><th colspan="2">LG</th><th colspan="2">HG</th></tr>
<tr><td rowspan="12">HL-60 and Jurkat</td><td colspan="3">Proliferation & viability assay</td><td colspan="2" rowspan="2">0.0 mM</td><td colspan="2" rowspan="2">0.0 mM</td><td colspan="2" rowspan="2">0.0 mM</td></tr>
<tr><td>24 h</td><td>48 h</td><td>72 h</td></tr>
<tr><td colspan="3" rowspan="2">Alamar Blue assay</td><td>0.0 mM</td><td>1.0 mM</td><td>0.0 mM</td><td>1.0 mM</td><td>0.0 mM</td><td>1.0 mM</td></tr>
<tr><td>0.1 mM</td><td>3.0 mM</td><td>0.1 mM</td><td>3.0 mM</td><td>0.1 mM</td><td>3.0 mM</td></tr>
<tr><td colspan="2">24 h</td><td>48 h</td><td>0.5 mM</td><td>5.0 mM</td><td>0.5 mM</td><td>5.0 mM</td><td>0.5 mM</td><td>5.0 mM</td></tr>
<tr><td colspan="3">BrdU assay</td><td>0.0 mM</td><td>1.0 mM</td><td>0.0 mM</td><td>1.0 mM</td><td>0.0 mM</td><td>1.0 mM</td></tr>
<tr><td colspan="3">48 h</td><td>0.1 mM</td><td>3.0 mM</td><td>0.1 mM</td><td>3.0 mM</td><td>0.1 mM</td><td>3.0 mM</td></tr>
<tr><td colspan="3" rowspan="2">Proliferation & viability assay with metformin</td><td colspan="2">0.0 mM</td><td colspan="2">0.0 mM</td><td colspan="2">0.0 mM</td></tr>
<tr><td colspan="2">0.1 mM</td><td colspan="2">0.1 mM</td><td colspan="2">0.1 mM</td></tr>
<tr><td colspan="3">48 h</td><td colspan="2">3.0 mM</td><td colspan="2">3.0 mM</td><td colspan="2">3.0 mM</td></tr>
<tr><td colspan="3">Flow cytometric studies</td><td rowspan="2">0.0 mM</td><td rowspan="2">3.0 mM</td><td rowspan="2">0.0 mM</td><td rowspan="2">3.0 mM</td><td rowspan="2">0.0 mM</td><td rowspan="2">3.0 mM</td></tr>
<tr><td colspan="3">48 h</td></tr>
<tr><td rowspan="2">Jurkat</td><td colspan="2" rowspan="2">Flow cytometric study on ROS</td><td>I phase 48 h</td><td colspan="4" rowspan="2"></td><td>0.0 mM</td><td>3.0 mM</td></tr>
<tr><td>II phase 48 h</td><td>0.0 mM</td><td>0.0 mM</td></tr>
</table>

CELL COUNTING

During routine maintenance and throughout the experiments, cells were counted using either hemocytometer and microscope or Muse Cell Analyzer (EMD Millipore Corporation/Merck KgaA, Germany). Prior to counting, cells were thoroughly mixed with the pipette to allow equal cell dispersion.

CELL COUNTING ON MUSE™ CELL ANALYZER

Cell numbers and viability determination on Muse™ Cell Analyzer was conducted using Count&Viability Assay Kit according to Count&Viability protocol [49]. 50 µL of cell

suspension was mixed with 450 µL Muse™Count&Viability Reagent in a tube, followed by 5 min incubation at RT. Prior to reading, samples were mixed with Vortex to provide equal cell dispersion [56].

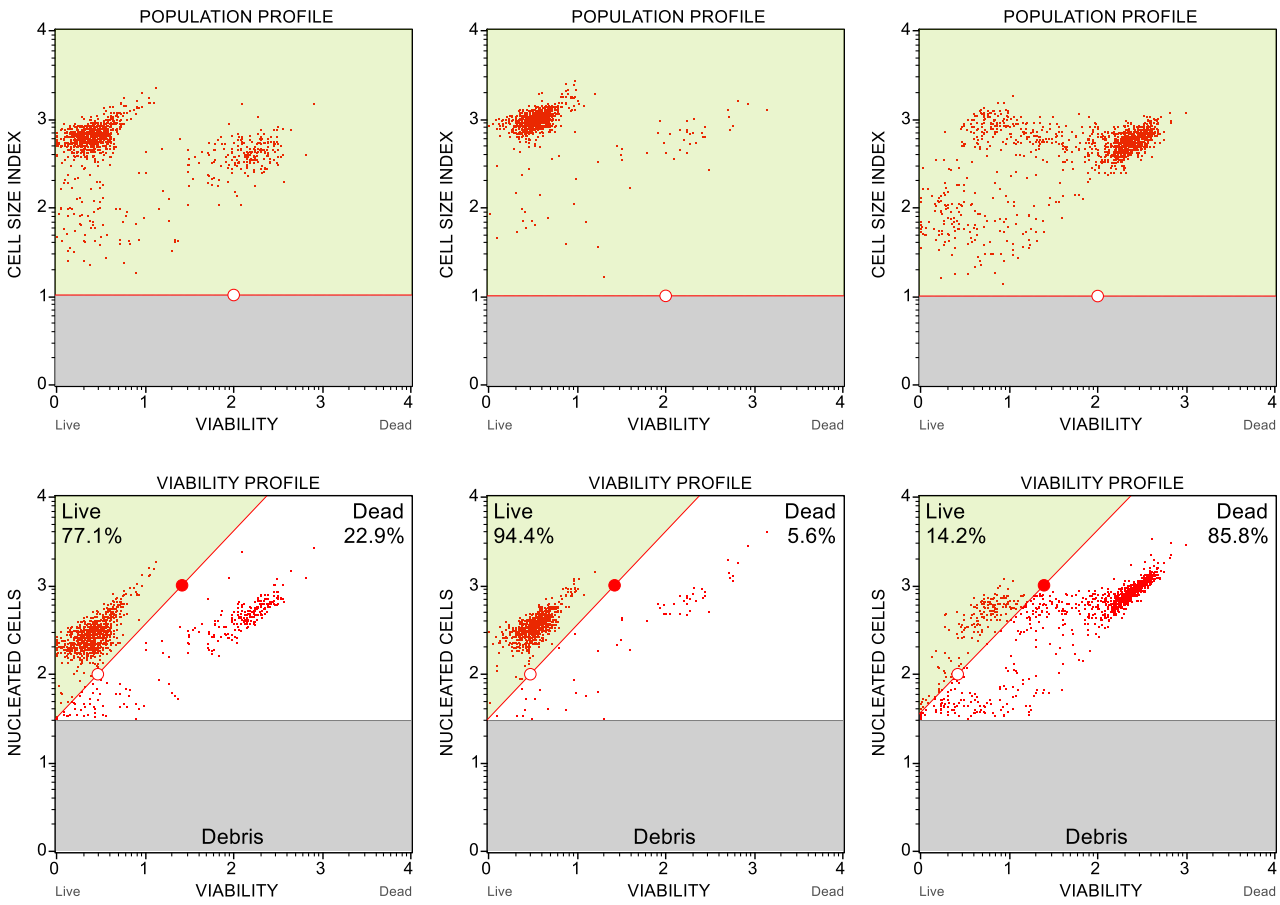

Figure 1 Overview on threshold settings in MUSE software. Population profile and viability profile of the same samples shown on the top and the bottom rows, accordingly. Left row presents Jurkat sample in NG 3.0 mM metformin treatment. Middle row shows HL-60 sample grown in NG 0.0 mM, while right row – in NG 3.0 mM metformin. Count & Viability assays were run after 48 h incubation.

Results were analyzed using Muse software [50]. The thresholds were set as indicated in **Figure 1**, with uniform CELL SIZE INDEX of 1.0 for VIABILITY vs CELL SIZE INDEX plot and minor threshold adjustments in VIABILITY vs NUCLEATED CELLS plot throughout the experiments to maintain separation between the viable and the dead cells populations. In the ambiguous cases the threshold was based on the settings valid for other samples of the same cell line.

PROLIFERATION ASSAY IN DIFFERENT GLUCOSE CONCENTRATION: NG, LG AND HG

Cells were seeded in the amount of 400 000 per well in 6-well plates in the total culture media volume of 3 mL. Cells were grown in RPMI 1640 medium with different glucose concentrations: HG, LG and NG, respectively. Cells were incubated for 24 h, 48 h and 72 h. Cells grown for 72 h were supplemented with 2 mL extra volume of the appropriate media after 48 h incubation.

After the incubation time, 1 mL of each cell suspension were taken and used for counting. Cell numbers and viability were determined using Count&Viability Assay Kit for Muse™ Cell Analyzer. pH of the cell suspension was also determined using test stripes.

ALAMAR BLUE PROLIFERATION ASSAY IN DIFFERENT GLUCOSE CONCENTRATION AND VARIOUS METFORMIN TREATMENT

Cells were seeded in 96-well black plate with clear bottom to minimize the scatter fluorescence while reading. 5000 cells were seeded in each well in a total suspension volume of 200 µL. Cells were grown in HG, LG and NG RPMI 1640 media in combination with different metformin concentrations: 0.0 mM, 0.1 mM, 0.5 mM, 3.0 mM and 5.0 mM respectively. Cells were incubated for 24 h and 48 h, respectively. 4 hours prior to the end of incubation period, each well has been added 20 µL of Alamar Blue reagent so that the final concentration in the well was 44 µM. The plates were protected from the excessive light exposure with an aluminum foil and put back in the incubator.

The fluorescence measurements were taken by SpectraMax®Paradigm®Multi-Mode Microplate Reader (Molecular Devices) at the excitation and emission wavelengths of

545 nm and 585 nm, respectively. Each measurement has been preceded by an instrument optimization run.

BrdU PROLIFERATION ASSAY IN DIFFERENT GLUCOSE CONCENTRATION AND VARIOUS METFORMIN TREATMENT

Experiment was conducted according to the protocol for Merc Millipore© BrdU Cell Proliferation Assay for suspension cells [51]. Leukemia cells were seeded with a starting number of 10 000 per well in 96-well black plate with clear bottom in a total volume of 200 µL. Cells were grown in HG, LG and NG RPMI 1640 media with different metformin concentrations of 0.0 mM, 0.1 mM, 1.0 mM and 3.0 mM, respectively. Two types of controls were also made: with media only, added BrdU reagent (blanks) and with cells present but not added the BrdU reagent (background). Cells were incubated for 48 h. 20 hours prior to the results reading, BrdU reagent has been added to each well in a volume of 20 µL, except from controls without BrdU reagent added.

After the incubation time, plate was spun down for 5 min at 1000 rpm with the centrifuge brake off. Medium was removed and Fixing Solution was added to each well in a volume of 200 µL. Plate was incubated for 30 min at RT. Then Fixing Solution was aspirated. Plate was washed 3 times with Wash Buffer, followed by blot drying with a paper towel. Detector antibody solution was added in a volume of 100 µL, followed by 1h incubation at RT. Then the plate was washed 3 times with Wash Buffer. The Goat anti-Mouse IgG, Peroxidase Conjugate solution was prepared and administered to each well in a volume of 100 µL, followed by 30 min incubation at RT. Then the plate was washed 3 times and flooded with distilled water, carefully blot dried. The TMB Peroxidase Substrate solution was pipetted into each well in a volume of 100 µL, followed by 30 min incubation at RT in the dark. After this time, 100 µL of the acid Stop Solution was added into each well.

The 96-well plate was read on SpectraMax®Paradigm®Multi-Mode Microplate Reader (Molecular Devices) using dual fluorescence wavelength of 450 nm and 550 nm as a reference.

PROLIFERATION ASSAY IN DIFFERENT GLUCOSE CONCENTRATION AND METFORMIN TREATMENT

Leukemia cells were seeded with the starting density of 400 000 cells per well in 6-well plates in a total media volume of 3 mL. Cells were grown in HG, LG and NG RPMI 1640 media with different metformin concentration, 0.0 mM, 0.1 mM and 3.0 mM, respectively. Cells were incubated in for 48 h.

Cell numbers were determined using the Count&Viability Assay Kit on Muse™ Cell Analyzer. pH of the cell suspensions was also determined using the test stripes.

METABOLIC PROFILING OF TWO LEUKEMIA CELL LINES IN DIFFERENT GLUCOSE CONDITIONS

Cells were seeded at starting number of 60 000 per well in 12-well plates and cultured in HG, LG and HG RPMI 1640 media in a total volume of 3 mL for 48 h prior to the Cell Energy Phenotype Test.

The day preceding the assay, the Sensor Cartridge was hydrated with Agilent Seahorse XF Calibrant according to the *How to Hydrate an Agilent Seahorse XFp Sensor Cartridge* procedure [52] and left in non-CO_2 incubator (VWR) at 37ºC overnight.

The supplemented assay medium was freshly prepared according to the *Preparation of XF assay media* protocol [53] for Cell Energy Phenotype Test as shown in the **Table 4**, followed by pH adjustment to 7.4 using 0.5 N NaOH and pH test stripes. Medium was warmed up to 37ºC.

Table 4 Supplementary reagents for XFp Assay Medium preparation [53].

REAGENT	Final concentration
Glucose	10 mM
Sodium pyruvate	1 mM
L-glutamine	2 mM

Prior to seeding procedure, the plate's wells were coated with Corning® Cell-TAK™ according to *Corning® Cell-TAK™ Cell and Tissue Adhesive Instructions for use: Coating Procedure for Multiple Well Plates* [54] and *Immobilization of Non-Adherent Cells with Cell-Tak for Assay on the Agilent Seahorse XFe/XF96 Analyzer* [55] protocols.

Cells were seeded according to *Immobilization of Non-Adherent Cells in Agilent Seahorse XFp Cell Culture Miniplates* protocol [55] on the Cell-Tak coated Seahorse XFp Cell Culture Miniplates with the density of 60000 cells/well.

Appropriate number of cells was resuspended in previously prepared assay medium and seeded in the volume of 50 µL. Blank wells were filled with equal volume of assay medium only. Plate was then centrifuged at 300 x g for 1 min with no braking. Adhesion of the cells was checked using the microscope. Plate was kept at 37ºC in non-CO_2 incubator (VWR) for 30 min. Then wells were re-examined with the microscope for the cell adhesion and carefully added 130 µL assay medium so that each well was filled with total volume of 180 µL. Plate was placed back in the non-CO_2 incubator (VWR) for another 20 minutes.

Stressor mix was prepared freshly according to Table 4 in the *Agilent Seahorse XFp Cell Energy Phenotype Test Kit* protocol [56] so that the port concentrations of FCCP and oligomycin concentrations were 10 µM. Appropriate ports of the Sensor Cartridge were filled with 20 µL of the stressor mix prior to calibration.

Seahorse XF Cell Energy Phenotype Test was run on Seahorse XFp Analyzer (Agilent Technologies). Three measurements of Baseline Oxygen Consumption Rate (OCR) and Baseline Extracellular Acidification Rate (ECAR) followed by the stressor mix injection and five measurements of Stressed OCR and Stressed ECAR were included in the assay. Results were analyzed using Wave 2.4.0 software with built-in Seahorse XF Cell Energy Phenotype Test Generator [57].

FLOW CYTOMETRY STUDIES ON METFORMIN EFFECT ON MITOCHONDRIAL PARAMETERS

DETERMINATION OF MITOCHONDRIAL MEMBRANE POTENTIAL, MITOCHONDRIAL QUANTITY AND ROS FORMATION UPON METFORMIN TREATMENT USING FLUORESCENT STAINING ASSAYS

Three flowcytometric assays were run to study MMP, mitochondrial content and ROS formation, using TMRM (Tetramethylrhodamine, Methyl Ester, Perchlorate), MTDR (MitoTracker™ Deep Red) and CM-H_2DCFDA staining assays, accordingly. General experimental procedures for all mentioned assays were the same, with differences regarding concentrations of the dyes, staining duration and optical filter settings, as indicated in the **Table 5**.

Table 5 Staining assays information and technical data for TMRM, MTDR and CM-H2DCFDA [58–60].

Staining assay/dye	TRMR	MTDR	CM-H2DCFDA
Assay target	MMP	Mitochondrial content	General ROS
Staining solution conc.	1 µM	100 nM	5 µM
Incubation time	30 min	30 min	15 min
Excitation/emission	548/574 nm	644/665 nm	492~495/ 517~527 nm
Fluorescence detector	FL2 585/40 nm	FL4 675/25 nm	FL1 533/30 nm

Prior to the assay, cells were seeded in the number of 1 000 000 per well in 12-well plates in 3 mL of HG, LG and NG RPMI 1640 media in combination with metformin concentration of 0.0 mM and 3.0 mM, respectively. Cells were incubated for 48 h.

The staining solution was freshly prepared using RPMI 1640 medium without glucose so that the final concentration of TMRM, MTDR and CM-H2DCFDA were 1 µM, 100 nM and

5 µM, respectively. Cells numbers were determined using hemocytometer. 200 000 cells were taken up into Eppendorf tubes, centrifuged at 800 rpm/4 min. Media were aspirated and cells were resuspended in 200 µL of TMRM, MTDR or CM-H2DCFDA staining solution, followed by 30 min, 30 min or 15 min incubation at 37ºC, accordingly (**Table 5**). The tubes were centrifuged at 800 rpm/3 min, the staining solution was aspirated, and the stained cells were washed with 100 µL PBS. Samples were kept on ice. Unstained samples were also prepared, skipping the staining step.

Samples were read using flow cytometer BD Accuri™ C6 Plus (BD Biosciences, USA). Fluorescence signal was recorded using optical emission filters FL2, FL4 or FL1 for TMRM, MTDR and CM-H2DCFDA staining, respectively (**Table 5**). Results were acquired using CFlow Plus software. Prior to data collection the population of viable cells was selected for desired data acquisition of 10000 events. Fluidics setup was chosen to the medium flow rate. Readings were taken within 1 hour after the staining procedure was finished. Results were analyzed using CFlow ®.

FLOW CYTOMETRY STUDY ON THE METFORMIN REMOVAL EFFECT ON JURKAT CELLS

Basing on the results obtained in previous flowcytometric experiment, formation of ROS in HG cultured Jurkat cells, treated with 3.0 mM metformin was further investigated, with extended incubation of the cells in HG medium upon metformin removal after 48 h, as illustrated in the diagram in **Figure 2**.

Jurkat cells were cultured for 48 h in 12-well plates in a total volume of media of 2 mL with the starting seeding number of 600 000 per well. Cells were grown in HG RPMI 1640 media in combination with metformin treatment of 0.0 mM and 3.0 mM, respectively.

After 48 h incubation, cells were counted using Muse™ Cell Analyzer. pH of the cell suspension media was measured using test stripes. 200 000 cells were taken into the tubes and used for staining procedures, CM-H2DCFDA, TMRM and MTDR, as previously described and illustrated in **Table 5**. TRMR and MTDR were prepared as one staining solution, due to the same incubation time. Measurements were recorded using flow cytometer BD Accuri™ C6 Plus (BD Biosciences, USA) as previously indicated (**Table 5)**.

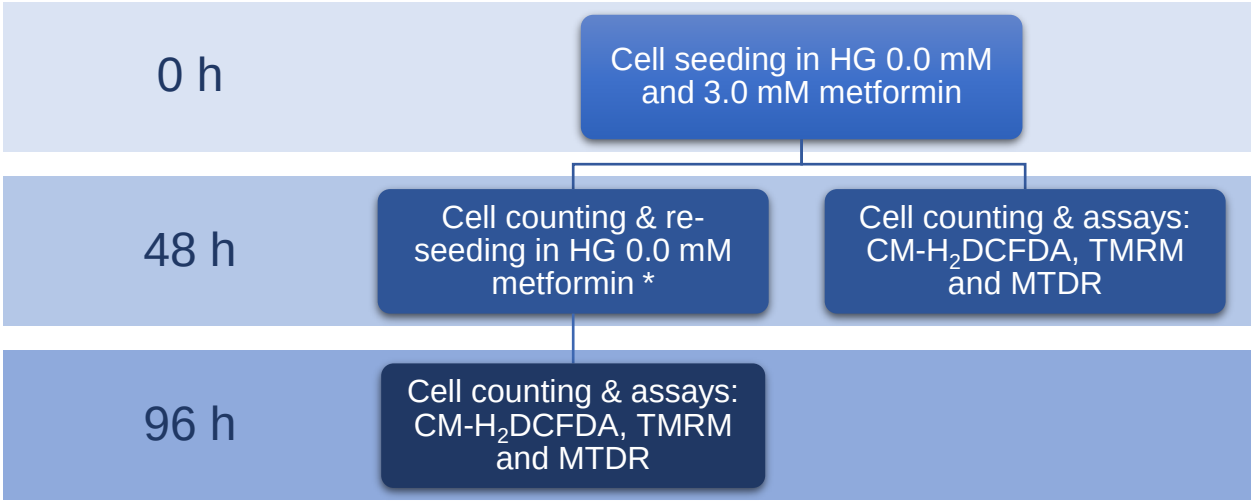

Figure 2 Metformin removal effect on ROS: experimental layout. Flowcytometric study on the metformin removal effect on mitochondria in Jurkat cells grown in HG condition. * indicates two variants of the experimental design: 1) all the cells were re-seeded for the further incubation and 2) cells were re-seeded in the amount equal to the starting seeding density.

Cells were also re-seeded in 12-well plates in 2 mL of the fresh HG RPMI 1640 without metformin upon removal of the previous media by centrifugation at 800 rpm/3 min. Cells formerly grown in 3.0 mM media were additionally washed twice with 1 mL HG RMPI 1640 prior to re-seeding. In the first attempt of the experiment, all cells were re-seeded, while in the second attempt, cells were re-seeded in the number equal to the starting seeding density to check if the results obtained in the first attempt were affected by high cell density after total of 96 h incubation. Cells were incubated for another 48 h. After this time, cells were counted on Muse™ Cell Analyzer, and the pH of cell suspension was checked using test stripes. CM-H2DCFDA, TMRM and MTDR staining assays and readings were conducted again as described above in this section.

STATISTICAL ANALYSIS

Statistical analysis was done in Microsoft Excel 2016 using student t Test for equal or unequal variances, as indicated by preceding F test, with the statistical significance of $p < 0.05$.

9. RESULTS

GLUCOSE DEPLETION SIGNIFICANTLY DECREASES THE PROLIFERATION RATE OF BOTH LEUKEMIA CELL LINES

To investigate the relation between glucose availability and HL-60 and Jurkat cells growth, the proliferation in different glucose growth conditions was conducted. Both cell lines exhibited accelerated growth under LG and HG conditions, with NG conditions being unfavorable for cell proliferation (**Figure 3, Figure 4**). Estimated doubling times for Jurkat cells were generally longer than HL-60 cells (**Table 6**). NG conditions caused an increase in doubling time by 65.94% and 56.66% for Jurkat and HL-60 cells, accordingly. Interestingly, doubling time was not significantly different for LG and HG conditions for both cell lines.

Table 6 Growth rate and doubling time in different glucose conditions. HL-60 and Jurkat cells were grown in HG, LG and NG. Calculations based on the data collected after 24h, 48h and 72h of incubation.

Glucose growth condition	HL-60		Jurkat	
	Growth rate	Doubling time [h]	Growth rate	Doubling time [h]
NG	0.0254	27.29	0.0191	36.29
LG	0.0375	18.48	0.0315	22.00
HG	0.0398	17.42	0.0317	21.87

To further investigate the impact of glucose on the cells, the viability was analyzed. A general trend for a slight viability decrease in NG condition for both cell lines was observed, especially when exposed to growth condition for 48 h and 72 h (**Appendix; Figure 19**).

Measurements of the media pH were higher in NG groups for both cell lines (**Appendix: Figure 18**).

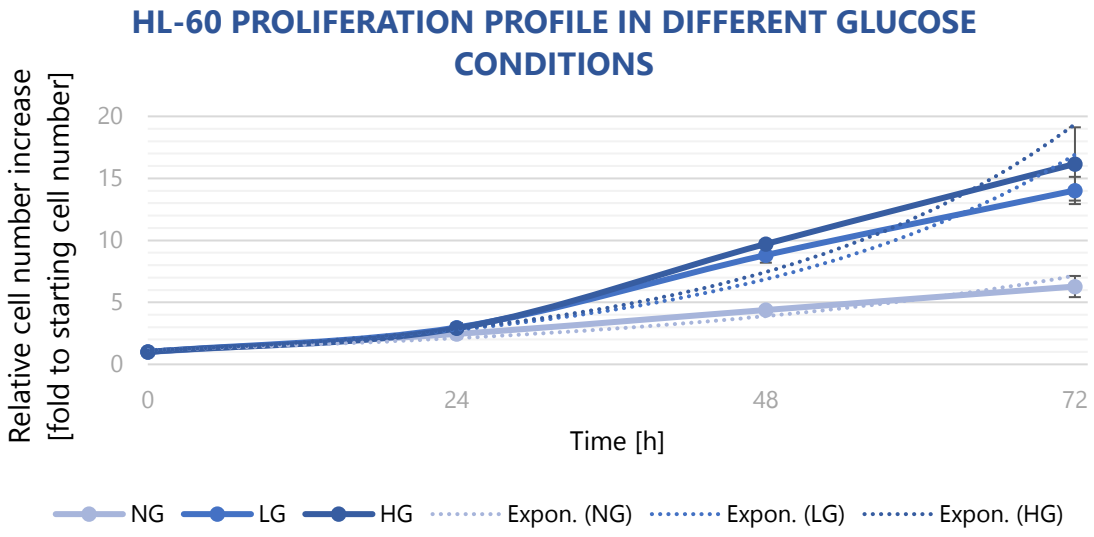

Figure 3 HL-60 proliferation in different glucose conditions. Cells were cultured in NG, LG and HG for 24h, 48h and 72h time periods. Exponential growth rate trends are shown in the graph as dotted lines. N=3.

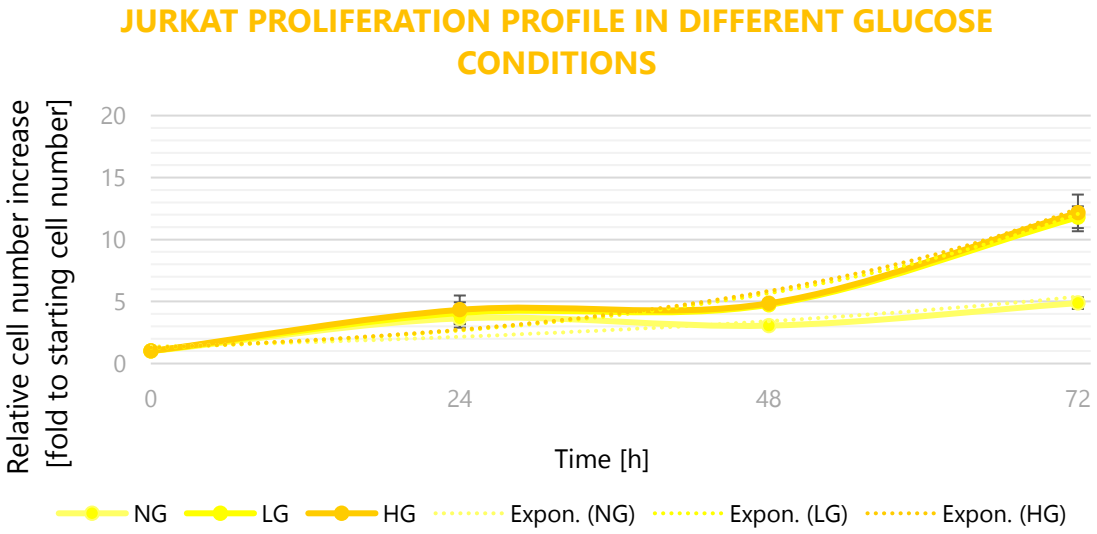

Figure 4 Jurkat proliferation in different glucose conditions. Cells were cultured in NG, LG and HG for 24h, 48h and 72h time periods. Exponential growth rate trends are shown in the graph as dotted lines. N=3.

GLUCOSE AVAILABILITY AFFECTS THE IMPACT OF HIGH METFORMIN DOSES ON PROLIFERATION IN BOTH CELL LINES

To determine the impact of metformin on the cell proliferation, two assays were run, based on different principles.

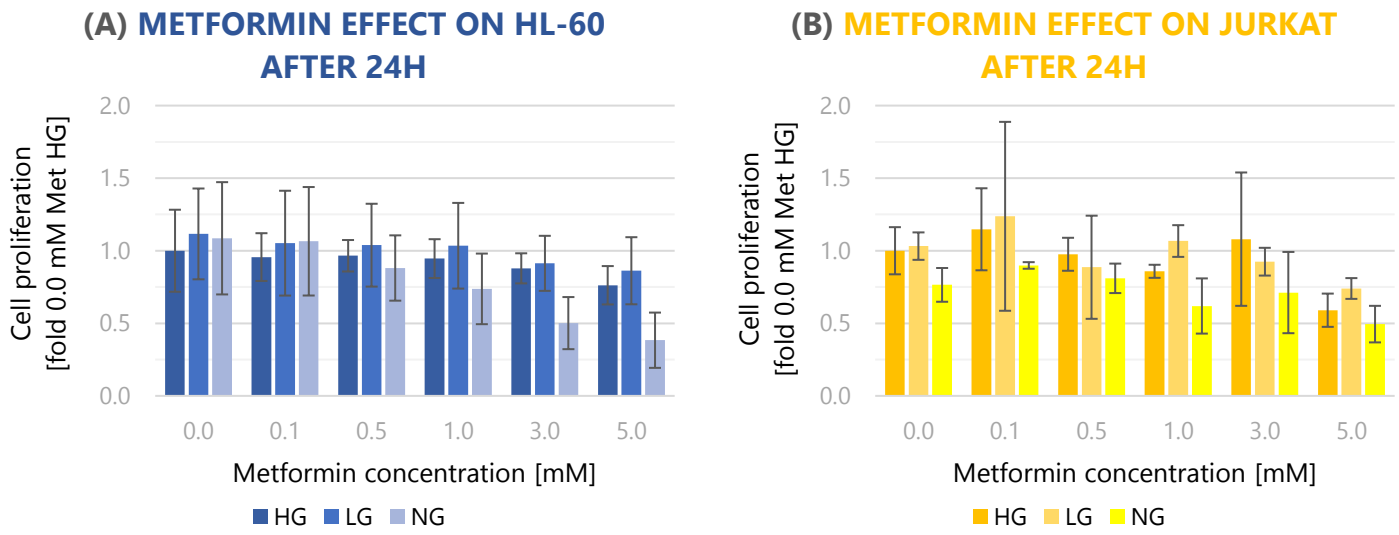

Figure 5 Alamar Blue proliferation assay results after 24h. HL-60 (A) and Jurkat (B) cells were grown in different glucose conditions: HG, LG and NG, and treated with metformin for 24h prior to the assay. Numbers normalized to 0.0 mM Met HG sample. N=3

After 24 h incubation with metformin, the viability decreases along with increasing metformin treatment concentration (**Figure 5**). In case of HL-60 cells, the effect of metformin after 24 h was the strongest in NG group treated with 3 mM and 5 mM (**Figure 5A).** LG and HG groups were not significantly responsive to the metformin treatment within range 0.1 mM – 1 mM, with the slight viability decrease in higher concentrations. In general, NG group exhibited the highest susceptibility to the metformin treatment.

Similar pattern was observed for Jurkat cells after 24 h incubation, with generally more responsiveness to the treatment at lower concentrations, especially in NG group (**Figure 5B**). There was an increase in viability for all glucose groups treated with 0.1 mM metformin. The only group that exhibited significant reduction in cell viability for all glucose growth conditions was the one treated with 5 mM metformin.

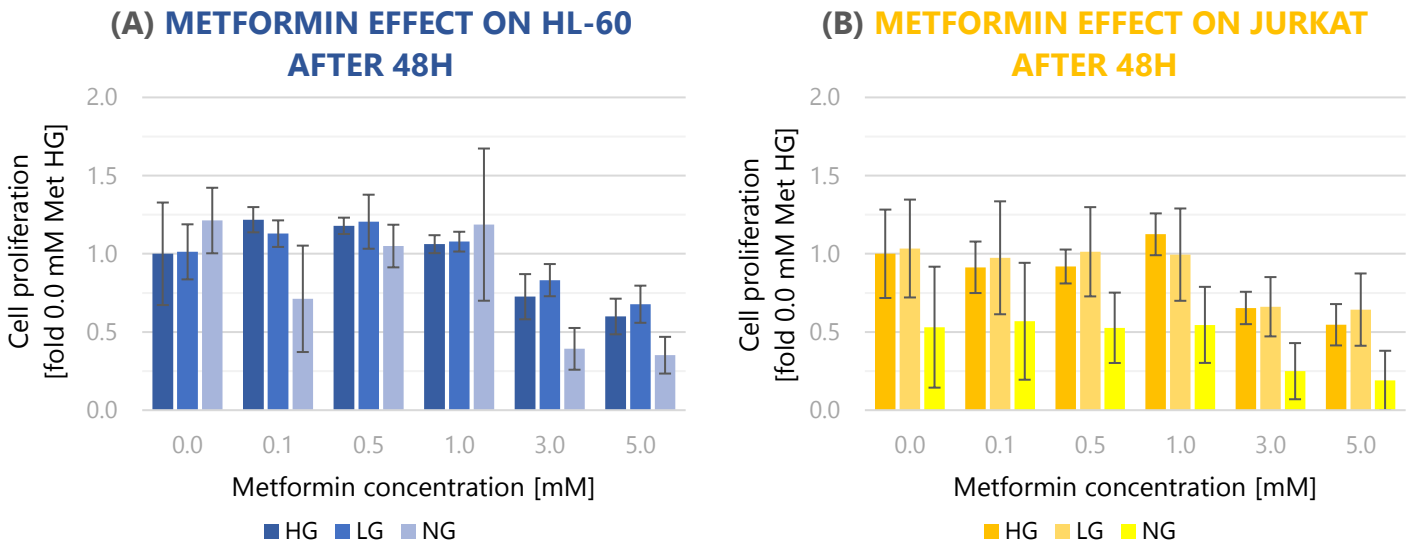

Figure 6 Alamar Blue proliferation assay results after 48h. HL-60 (A) and Jurkat (B) cells were grown in different glucose conditions and treated with metformin for 48h prior to the assay. Numbers normalized to 0.0 mM Met HG sample. N=3

More pronounced effect of metformin was seen after 48 h. A common pattern of significant viability reduction for the cells treated with 3 mM and 5 mM was observed, especially in NG group and generally more severe in Jurkat cell line (**Figure 6**). There was nearly any effect of the drug within the concentration range of 0.1 mM to 1.0 mM. Interestingly, Jurkat viability levels were identical for 3.0 mM and 5.0 mM treated LG and HG groups, as well as NG cells that received no or 0.1 mM – 1.0 mM drug.

HIGH METFORMIN DOSES SIGNIFICANTLY REDUCE PROLIFERATION OF GLUCOSE DEPLETED LEUKEMIA CELLS

The second proliferation assay, BrdU, is based on incorporation of fluorescent molecule into actively proliferating cell's DNA.

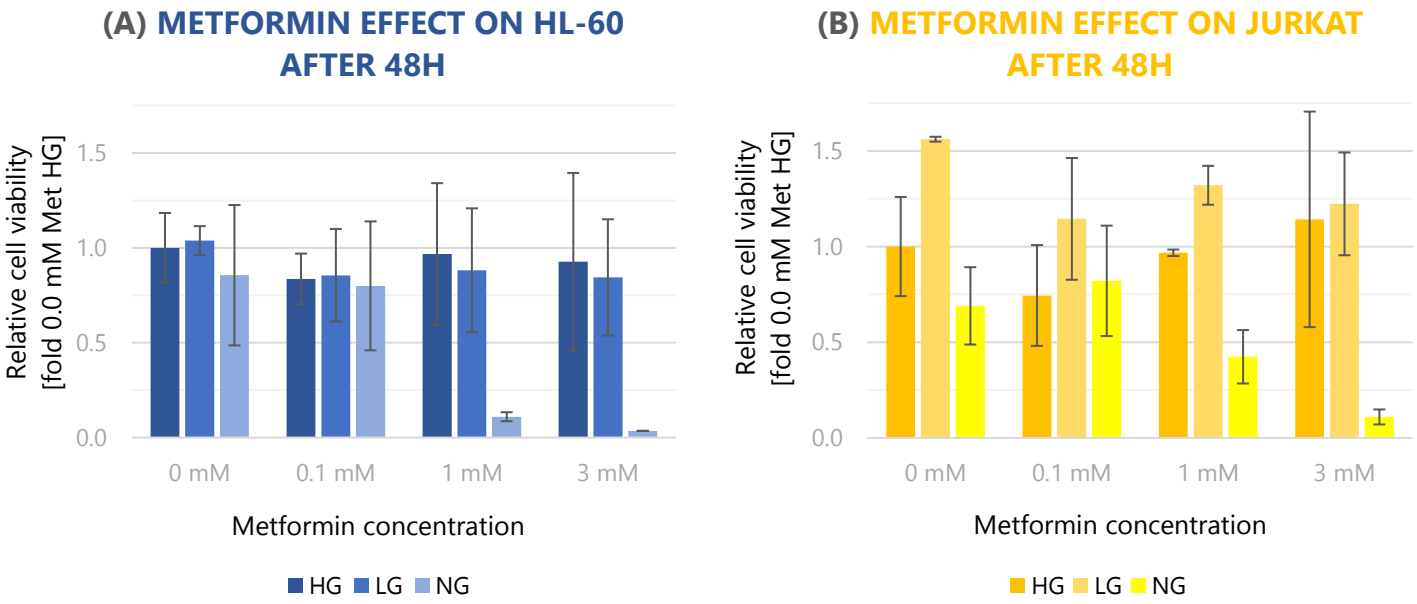

Figure 7 Metformin effect on cell proliferation: BrdU Assay. HL-60 (A) and Jurkat (B) cells after 48h 0.0 mM, 0.1 mM, 1.0 mM and 3.0 mM metformin treatment in HG, LG and NG. Numbers normalized to 0.0 mM Met HG group. Standard deviation shown as the error bars. N=2

In HL-60 cell line, significantly reduced viability of 0.11 and 0.04 was observed only in NG grown cells treated with 1 mM and 3mM metformin, respectively (**Figure 7A**). The same groups exhibited the lowest viability recorded in Jurkat, with values of 0.42 and 0.11, accordingly (**Figure 7B**). There was no notable effect of neither glucose concentration nor metformin in other experimental groups of HL-60 (**Figure 7A**). Jurkat cells showed the general trends of a relatively the highest viability in LG and a decreased viability in NG groups throughout all metformin treatments, respectively (**Figure 7B**).

There was slight discrepancy noted between the results obtained via Alamar Blue and BrdU assays. HL-60 cells grown in HG and LG conditions that received 0.1 mM metformin treatment expressed reduced proliferation of 0.84 and 0.86 in BrdU test, respectively, (**Figure 7A**), while the same groups showed increased proliferation of 1.22 and 1.13 in Alamar Blue assay (**Figure 6A**). Also, for 1 mM treated glucose depleted HL-60 cells 1.19-fold increase (**Figure 6A**), but 0.11-fold reduction (**Figure 7A**) of proliferation was observed in Alamar Blue and BrdU test results, respectively. In 3 mM metformin treated Jurkat cells grown in HG and LG, 0.65-fold and 0.66-fold reduction (**Figure 6B**) in Alamar Blue was found, but 1.14-fold and 1.22-fold increase in BrdU was noted (**Figure 7**).

The discrepancy of the results obtained in the assays is directly attributed to the different principles they rely on. Alamar Blue employs resazurin, a redox dye, which upon cellular uptake is reduced into fluorescent form, resofurin, by oxidoreductase and electrons from NAD(P)H [45, 61]. Therefore, it reflects the state of metabolic activity of the cell. The second assay is based on incorporation of the fluorescent thymidine analog, BrdU, into *de novo* synthesized DNA of the actively proliferating cells during the S-phase [61]. Hence, despite of inconsistency of the results, they provide a comparative information on two aspects of metformin impact on the cell condition.

Of a general note, it appears that metformin requires the appropriate incubation period for the cellular metabolic response to be established. 24 h exposure to the drug exerts an effect, that could be described as “preliminary” or “provisional”, however, more clear influence is observed only after 48 h (**Figure 5, Figure 6**), which was then applied in the further experiments.

HIGH METFORMIN DOSE REDUCES PROLIFERATION REGARDLESS OF GLUCOSE CONCENTRATION AND AFFECTS VIABILITY OF THE CELLS

To establish the effect of selected 0.1 mM and 3.0 mM metformin doses, the proliferation and cell viability was studied.

High-dose metformin treatment significantly reduced the proliferation in both cell lines, with the most pronounced effect in glucose depleted groups. The reduction was substantially higher for HL-60 cells than Jurkat, with 92.86% and 63.77% decrease, respectively. There was no impact of 0.1 mM metformin treatment observed for both HL-60 and Jurkat cells. Regardless of metformin treatment, HL-60 proliferation was slightly enhanced by higher glucose concentration, which was not observed in Jurkat. Interestingly, in both cell lines, high metformin dose in glucose provided cells exhibited about the same reduction as for glucose depleted control (**Figure 8**).

Notable metformin impact on the cell viability was observed only in glucose depleted HL-60 and Jurkat cells treated with high dose metformin, with the cell viability reduction of 85.88% and 17.41% in comparison to NG control, accordingly (**Appendix: Figure 21, Figure 22**).

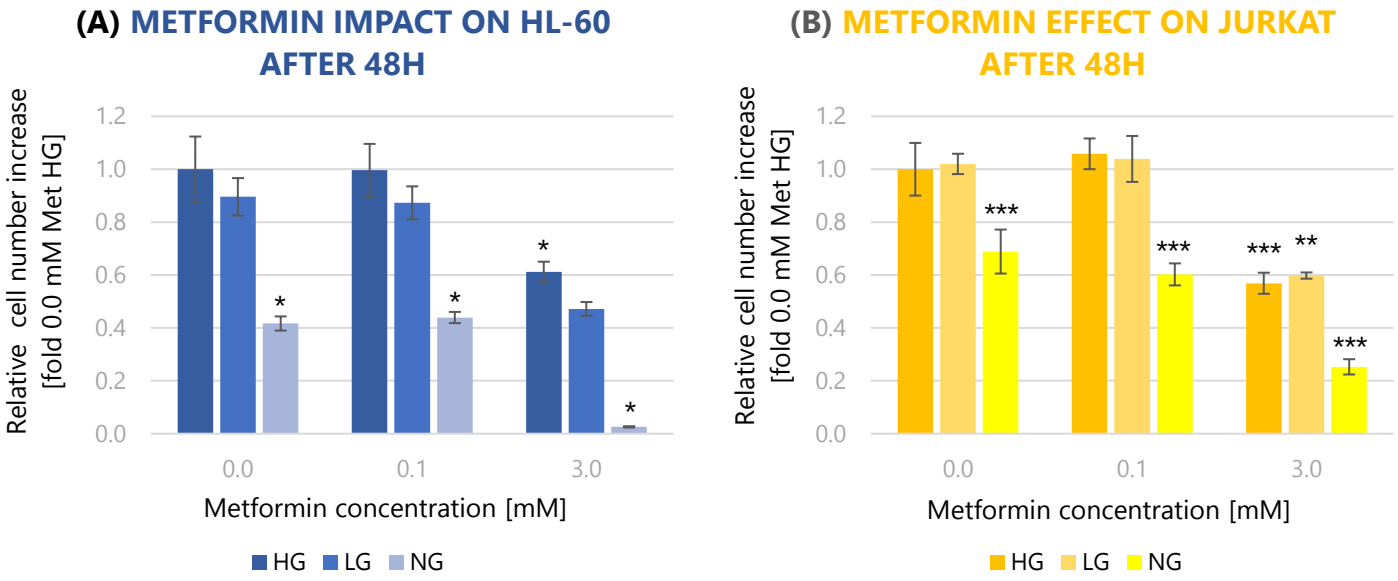

Figure 8 Metformin impact on cell proliferation after 48h. HL-60 (A) and Jurkat (B) were grown with metformin treatment: 0.0 mM, 0.1 mM and 3.0 mM in different glucose growth conditions for 48h. Based on viable cell numbers. Numbers normalized to 0.0 Met HG sample. N=3. *p<0.0001; **p<0.05; ***p<0.00001.

Media pH for HL-60 cell line showed gradual decrease with increasing glucose concentration, regardless of the metformin treatment. There was no or very little effect of metformin on the final pH of the media (**Appendix: Figure 20A**). For Jurkat cell line, there were nearly any changes in pH of the media observed (**Appendix:Figure 20B**).

HL-60 AND JURKAT EXHIBIT DIFFERENT METABOLIC PHENOTYPES AND ADAPT TO CHANGING GLUCOSE AVAILABILITY

To examine the metabolic changes of HL-60 and Jurkat cell lines in a response to different glucose conditions, a series of Cell Energy Phenotype tests were conducted using Agilent Seahorse XFp Analyzer. After exposure of the cells to HG, LG and NG conditions for 48 h, the oxygen consumption rate (OCR) and extracellular acidification rate (ECAR) were measured to reflect the mitochondrial respiration and glycolysis, accordingly. The measurements were taken before and after the parallel injection of oligomycin (ATP-synthase inhibitor) and FCCP (uncoupling agent) and treated further as baseline and stressed cell energy phenotype. Baseline and stressed phenotypes represent the

metabolic behavior of the cells under normal conditions of unlimited substrates, and under stressor-induced higher energy demand, respectively, and the difference between these two constitutes metabolic potential of the cell.

The results were presented in three different graphs: 1) Energy Map, showing the metabolic shift upon the stress (**Figure 9**), 2) Metabolic Potential, illustrating the stressed-induced change of OCR and ECAR in relation to Baseline values (**Figure 10**) and 3) Contribution of mitochondrial respiration and glycolysis in energy production in Baseline and Stressed conditions (**Figure 11**).

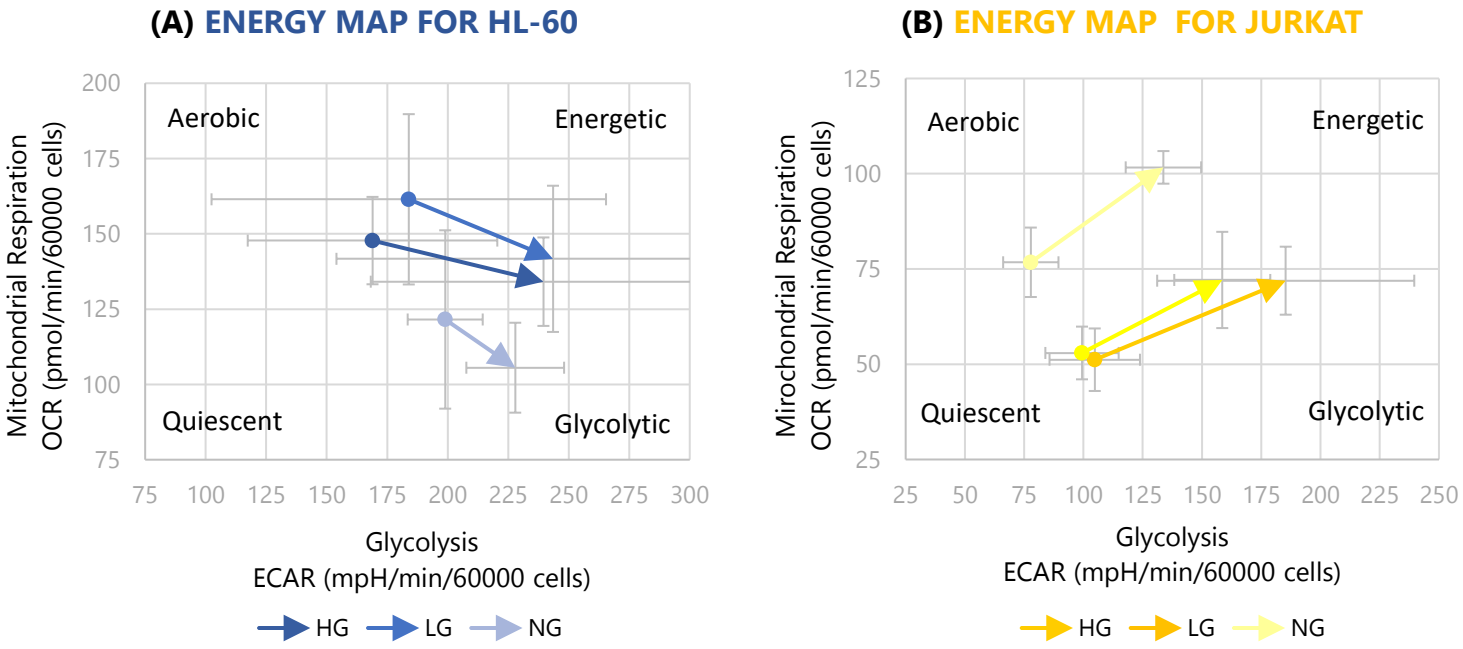

Figure 9 XFp Cell Energy Phenotype Test: Energy Map. Results for HL-60 (A) and Jurkat (B) cell lines. Cells were grown in HG, LG or NG conditions for 48h prior to the assay. Metabolic shift from Baseline Phenotype to Stressed Phenotype indicated with the arrow. Numerical values normalized to the seeding density of 60 000 cells per test well. N=3

HL-60 and Jurkat cell lines behaved differently in a response to mitochondrial stress. Metabolic shifts after HG, LG and NG 48 h growth conditions within the same cell line showed similar patterns, with HL-60 switching from aerobic towards glycolytic, while Jurkat from quiescent towards energetic metabolic profile (**Figure 9**).

Both cell lines expressed increase in ECAR levels under stressed conditions, with higher increase for Jurkat cell line. Regardless of preceding glucose growth conditions, there was a decrease and an increase in stressed OCR observed for HL-60 and Jurkat, respectively (**Figure 9**). The percentage values are presented in the graphs below (**Figure 10, Figure** 11).

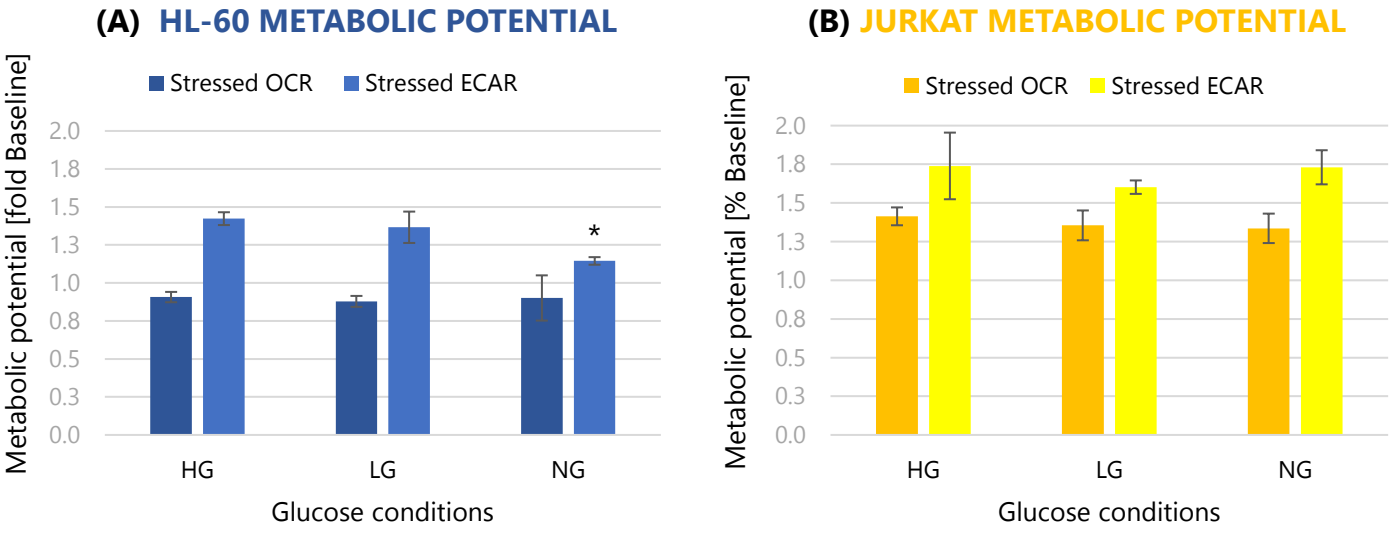

Figure 10 XFp Cell Energy Phenotype Test: Metabolic Potential. Results for HL-60 (A) and Jurkat (B) cell lines. OCR and ECAR values presented in relation to the baseline (100%). N=3.*p<0.01

Similar metabolic potentials in terms of mitochondrial respiration (% Baseline OCR) and glycolysis (% Baseline ECAR) were noted within each cell line, regardless of glucose pre-treatment, with only exception for significant decrease in Stressed ECAR for NG grown HL-60 cells (**Figure 10**).

Both cell lines showed higher OCR/ECAR ratios for baseline than the stressed condition (**Figure 11**). The OCR/ECAR values for HG and LG were higher than for NG condition in HL-60 cell line (**Figure 11A**). The opposite was seen in case of Jurkat cells, which had higher OCR/ECAR ratio for NG conditions (**Figure 11B**). Interestingly, the ratios for HG and LG conditions were of similar values both for HL-60 and Jurkat cells.

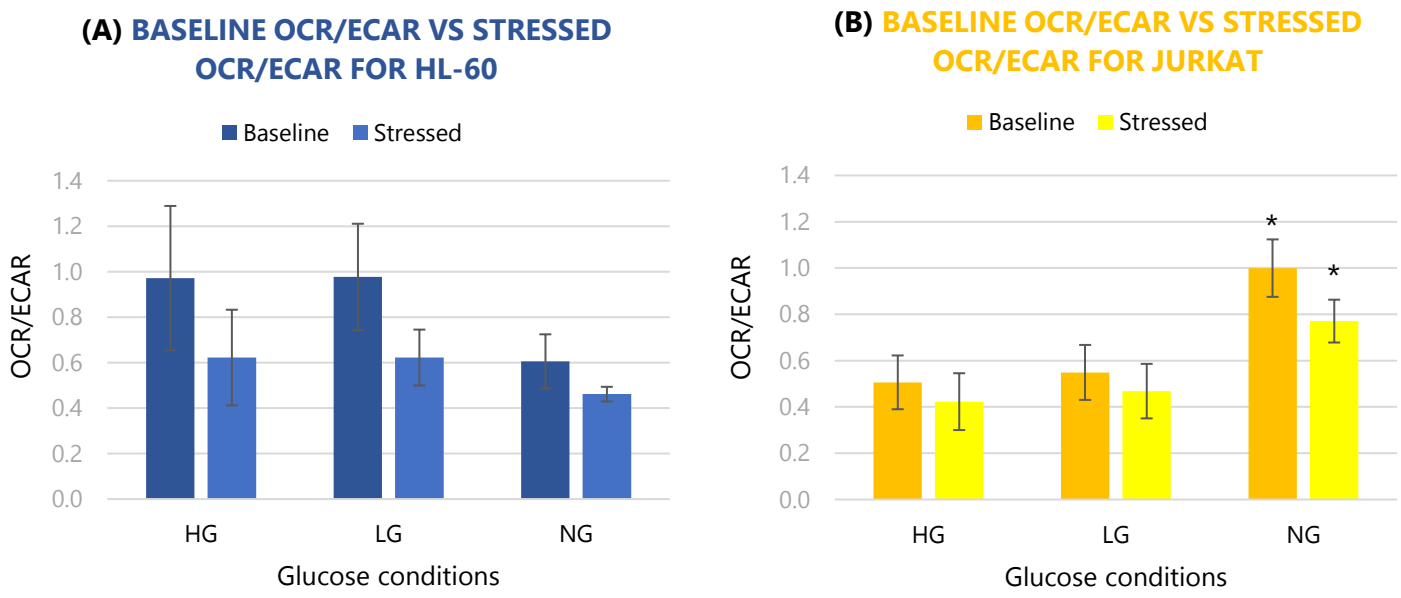

Figure 11 XFp Cell Energy Phenotype Test: Respiration vs Glycolysis. OCR/ECAR ratios for HL-60 (A) and Jurkat (B) cells grown in different glucose conditions for 48h prior to the assay. N=3. * p<0.05.

FLOW CYTOMETRY STUDIES ON VARIOUS MITOCHONDRIAL PARAMETERS

METFORMIN DECREASES THE MITOCHONDRIAL MEMBRANE POTENTIAL IN LEUKEMIA CELL LINES

TMRM staining assay was performed to study whether glucose growth conditions and high metformin dose have impact on MMP. Assay bases on accumulation of the dye in mitochondria of life cells upon present MMP.

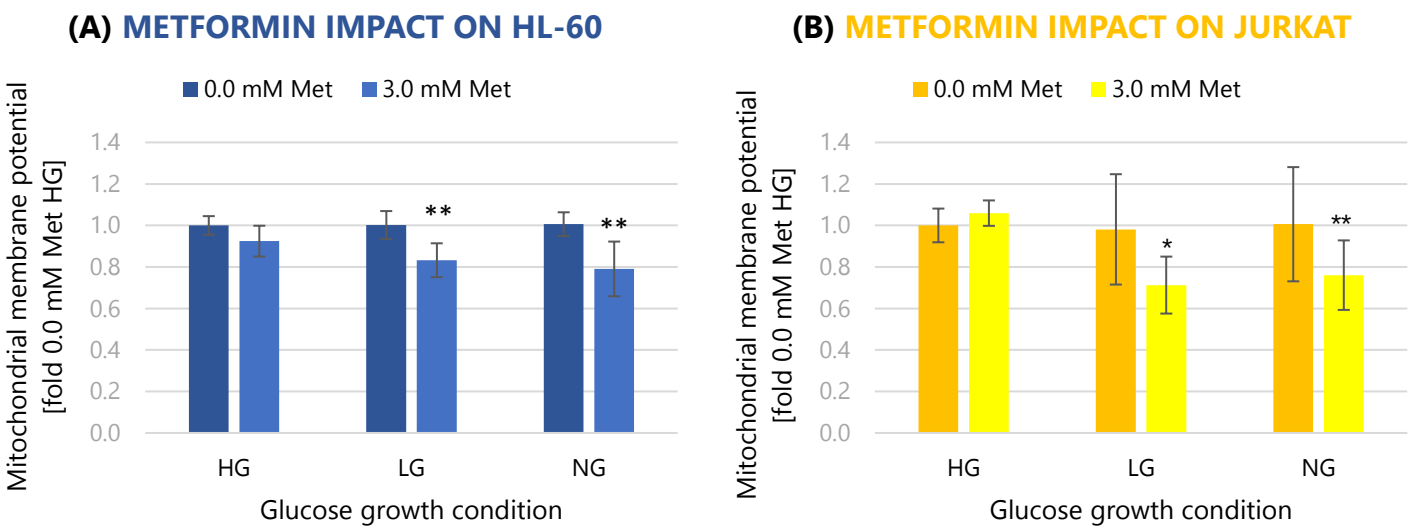

Figure 12 Metformin effect on MMP. Flow cytometry study on 3.0 mM metformin effect on mitochondrial membrane potential (MMP) for HL-60 (A) and Jurkat (B) cell lines. Cells were grown in HG, LG and NG conditions for 48h prior to the assay, with 0.0 mM or 3.0 mM metformin treatment. Median height FL2 data set normalized to 0.0 mM Met HG sample. N=3. *p<0.01; **p<0.001.

There was no effect of glucose growth condition on the MMP change observed for the cells of both lines that did not receive metformin treatment. In contrary, 3.0 mM metformin was shown to have moderate influence on MMP. The MMP-reducing effect of the drug was observed in LG and NG growth conditions for both cell lines (**Figure 12**), slightly more pronounced in Jurkat cells. Also, slight MMP increase was noted in this cell line for metformin treated cells in HG condition (**Figure 12B**).

THE NUMBER OF MITOCHONDRIA STAYS UNCHANGED UPON METFORMIN TREATMENT IN LEUKEMIA CELLS

MTDR assay was conducted investigate whether biogenesis of mitochondria is affected by glucose and metformin treatment. MTDR is also accumulated within mitochondria upon their MMP. The dye contains a reactive group which binds to proteins after the mitochondrial uptake.

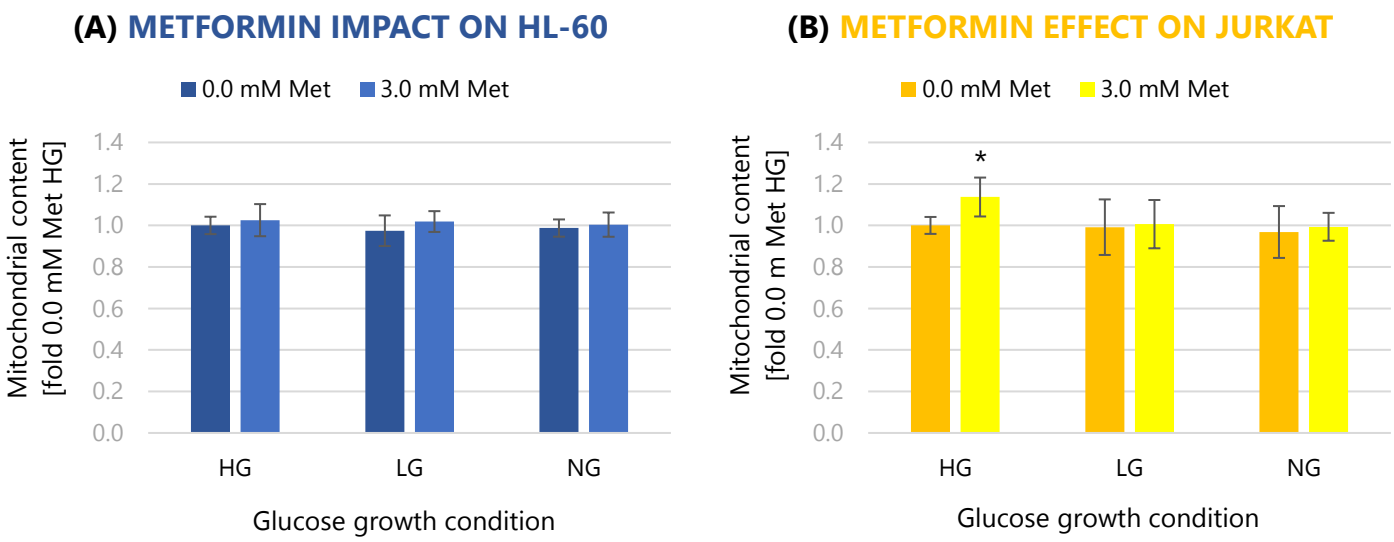

Figure 13 Metformin effect on mitochondrial content. Flow cytometry examination of the effect of 3.0 mM on the number of mitochondria in HL-60 (A) and Jurkat (B) cell lines. Cells were grown in HG, LG and NG conditions for 48h prior to the assay, with 0.0 mM or 3.0 mM metformin treatment. Median height FL4 data set normalized to 0.0 mM Met HG sample. N=3. *n=9; p<0.05.

After 48 h incubation, the MTDR signals were of the same values, regardless of either glucose growth conditions or metformin treatment (**Figure 13**). The only experimental group that showed a slight increase by 13.96% in comparison to 0.0 mM HG, were HG grown Jurkat cells treated with 3.0 mM metformin (**Figure 13B**).

GLUCOSE AND METFORMIN TREATMENT EXERT DIFFERENT IMPACT ON REACTIVE OXYGEN SPECIES FORMATION IN TWO LEUKEMIA CELL LINES

CM-H_2DCFDA assay was employed to measure the level of ROS, oxidative stress indicators, upon metformin treatment in different glucose growth conditions.

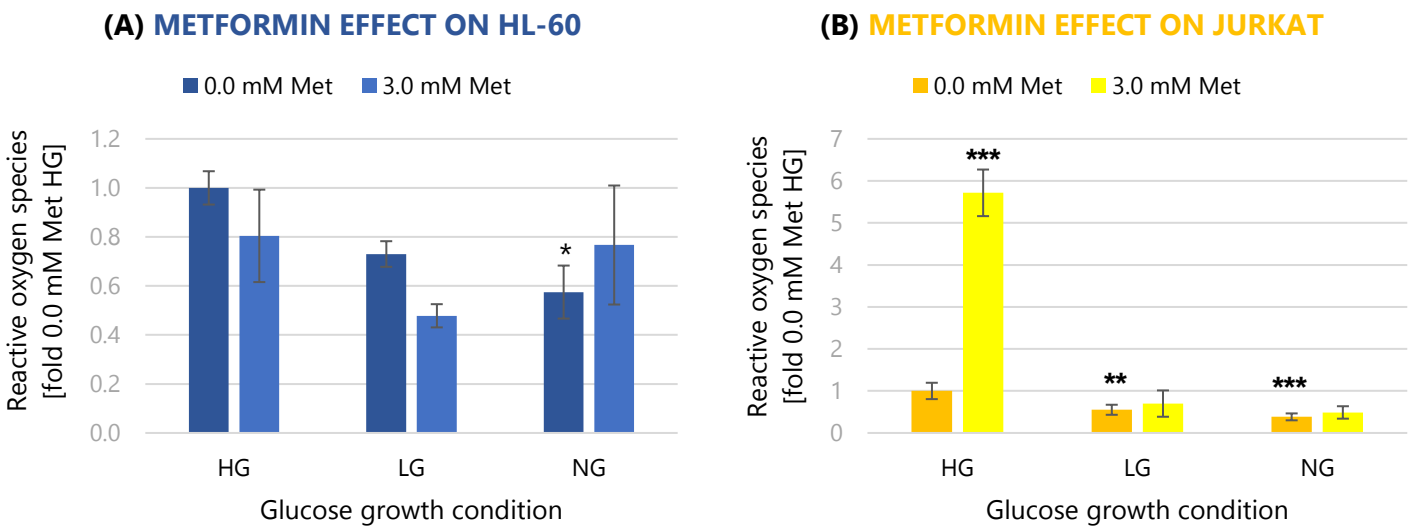

Figure 14 Metformin effect on ROS levels. Flow cytometry assay on the metformin influence on reactive oxygen species (ROS) formation in HL-60 (A) and Jurkat (B) cells upon 48h treatment with 3.0 mM in HG, LG and NG. Height median data set normalized to 0.0 mM Met HG sample. N=3. *p<0.05, **p<0.01, ***p<0.001.

Different glucose growth conditions, as well as metformin treatment, exerted an influence on ROS levels within the cells with the cell line specific response. Both cell lines exhibited general pattern of reduced ROS levels with decreasing glucose concentration (**Figure 14**). In HL-60 cells, metformin had further decreasing impact in glucose provided, but not in glucose depleted cells, where an increase of ROS level was observed (**Figure 14A**). In Jurkat cells, metformin caused elevated ROS levels in all groups, with notably higher increase in HG grown cells (**Figure 14B**).

ROS LEVELS IN HG GROWN JURKAT CELLS ARE BROUGHT BACK TO NORMAL UPON METFORMIN TREATMENT DISCONTINUATION

As seen in the previous study, the levels of ROS in Jurkat cells after 48 h treatment with 3.0 mM metformin in HG condition were notably increased (**Figure 14B**). Therefore, removal of the metformin was introduced in this experiment to investigate the further response of the cells in terms of ROS formation. Experiment was run in two variants, first, with re-seeding all the cells after 48 h incubation, and based on the results obtained (**Figure 15A**), the re-seeding was adjusted to starting seeding cell number to investigate whether ROS levels were associated with high cell density.

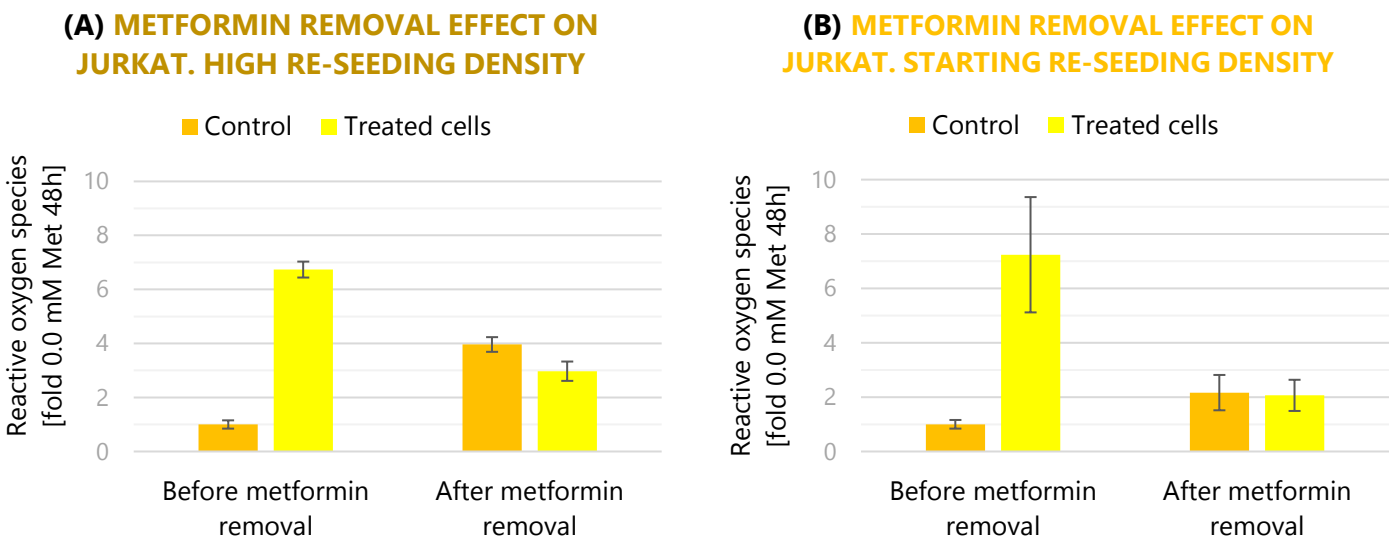

Figure 15 Metformin removal effect on ROS levels. The effect of metformin removal on the change in ROS levels in HG grown Jurkat cells. Two graphs represent the same experiment run in two variants: (A) cells re-seeded in full density after 48 h; (B) cells re-seeded in starting density after 48 h. N=3.

In the first attempt of the experiment, with high reseeding number of cells, a notable 3.96-fold increase in the ROS level in the untreated cells after 96 h was shown (**Figure 15A**). After reducing the re-seeding density, the ROS level was lower (2.16-fold) (**Figure 15B**).

Both variants of the experiment confirmed the increase in ROS levels after 48 h 3.0 mM metformin exposure, with 6.74-fold and 7.24-fold, as compared with untreated cells. After additional 48 h incubation upon metformin removal, ROS decreased by 51.93% and 71.55%, accordingly (**Figure 15**). Interestingly, in the second variant of the study, the ROS levels observed after 96 h were nearly the same for both untreated cells and the cells previously treated with 3.0 mM metformin, with 2.16 and 2.06-fold, respectively (**Figure 15B**).

After first phase of the experiment, the control and 3.0 mM metformin treated groups showed 2.48 and 1.48 fold increase in cell number, respectively. After second phase cell numbers for the same groups increased by 2.58 and 1.89 fold, accordingly (data only for the second variant of the experiment; **Appendix: Table 7, Table 8**).

There was no effect of metformin on cell viability observed, neither after first nor second phase of the experiment, with 96.4% and 96.9%, and 96.2% and 95.9% viability for untreated and treated cells, respectively (data only for the second variant of the experiment; **Appendix: Table 7, Table 8**).

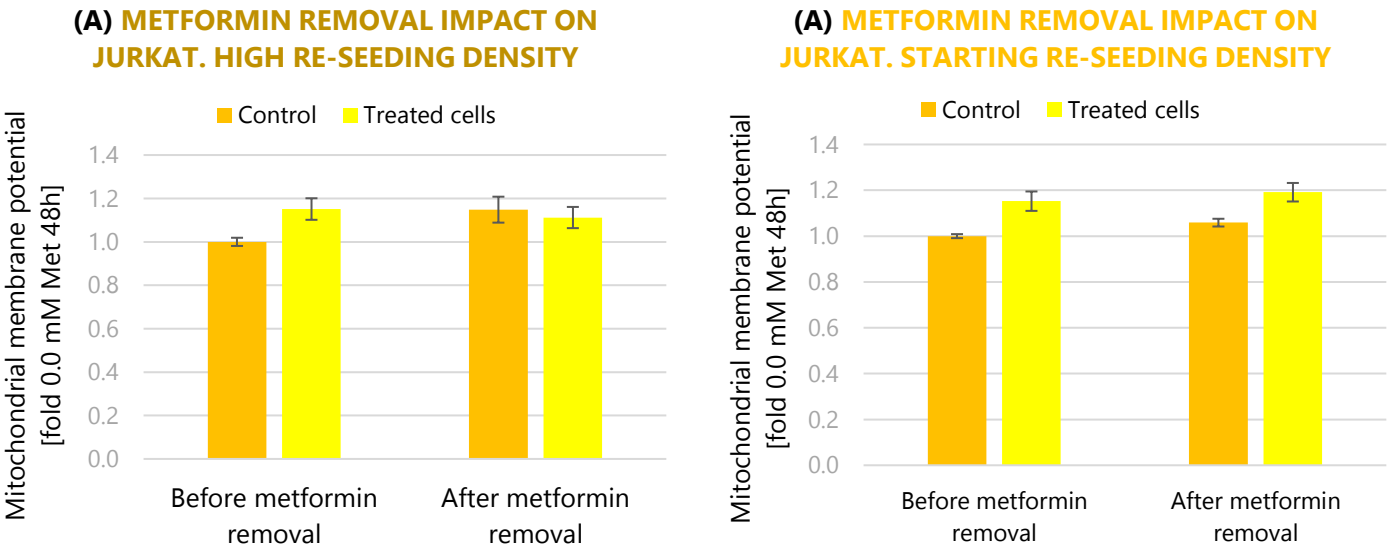

Figure 16 Metformin removal effect on MMP. MMP in Jurkat cells grown in HG condition before and after removal of 3.0 mM metformin treatment. Two graphs represent the same experiment run in two variants: (A) cells re-seeded in full density after 48 h; (B) cells re-seeded in starting density after 48 h. Data presented in (B) includes only 1 biological replicate for 96 h samples due to instrumental problems during the experiment.

The MMP results after 48 h (**Figure 16A**) were consistent to the previous study (**Figure 12B**) and showed a slight increase in the membrane potential (1.15-fold in both experiment variants). There was no significant change in MMP before and after metformin removal observed (**Figure 16**).

The MTDR assay showed moderately increased mitochondrial content after 48 h incubation with 3.0 mM metformin (**Figure 17A**), as seen in the previously presented results (**Figure 13B**). After metformin removal, the mitochondrial mass was reported to be of nearly the same value as seen for the untreated cells (**Figure 17**), with relative decrease and increase in the first and the second variant of the study, accordingly.

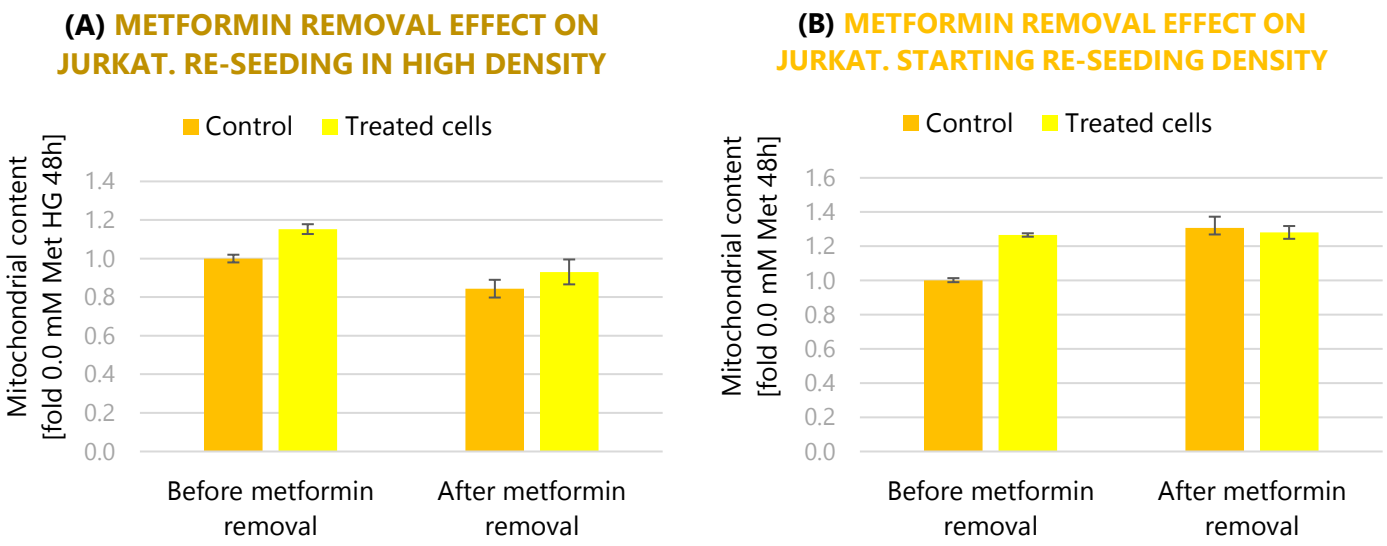

Figure 17 Metformin removal effect on mitochondrial biogenesis. Mitochondrial biogenesis in Jurkat cells grown in HG condition before and after removal of 3.0 mM metformin treatment. Two graphs represent the same experiment run in two variants: (A) cells re-seeded in full density after 48 h; (B) cells re-seeded in starting density after 48 h. Data presented in (B) includes only 1 biological replicate for 96 h samples due to instrumental problems.

Regarding the TMRM and MTDR results, it has to be borne in mind that due to different experimental conditions used in two attempts of the test, the comparative analysis of the results bears high risk of misinterpretation. Also, the instrumental issues during the analysis of TMRM and MTDR which led to possibility of reading only one biological sample, does not have informational value. Finally, the staining technique for TMRM and MTDR, performed as described in **FLOW CYTOMETRY STUDY ON THE METFORMIN REMOVAL EFFECT ON JURKAT CELLS**, implied a risk of the interference between two dyes, leading to falsified measurements.

10. DISCUSSION

The differential glucose growth conditions as a factor imposing the metabolic adaptation on two leukemia cell lines was the main objective of this study. Efficient mitochondrial respiration may represent an advantage in terms of metabolic flexibility. However, this advantage may be turned into a weakness when causing mitochondrial metabolism impairment with mitochondrial targeted drugs. In this study, metformin, a direct C–I inhibitor and depolarizing agent, was used to evaluate the ability of the cells to withstand the metabolic stress, correspondingly manifested in altered proliferation, viability and mitochondrial function. Two leukemia cell lines, known and confirmed in this study to possess distinct metabolic phenotypes, indicated the importance of endogenous cellular capabilities on the response to the metabolic stressor.

GLYCOLYTIC JURKAT CELL LINE ADAPTS TO GLUCOSE DEPLETION VIA METABOLIC SHIFT TOWARDS OXPHOS

Metabolic phenotyping of Jurkat cells revealed their high glycolytic capability [45]. Exposure to glucose depletion induced adaptative response in Jurkat cells activating OXPHOS to compensate lack of substrate to fuel glycolytic pathway [62]. Increase in OCR in Jurkat cells may imply that mitochondrial respiration systems in normal conditions are not fully exploited, which is reflected by spare capacity revealed upon stress (**Figure 9B, Figure 10B, Figure 11B**), which indicates presence of functional mitochondria in these cells [45].

HIGH OXIDATIVE METABOLISM POTENTIAL OF HL-60

Lack of OCR increase in the stressed phenotype of HL-60 cells, known to possess oxidative metabolism of higher efficiency than Jurkat [45], was an unexpected observation (**Figure 9A**). Unpublished study by J. Nikolaisen, performed on both cell lines, showed significantly higher oxidative capabilities of HL-60. The results can be explained by methodological issues and experimental design. The method used in the study supplies limited amount of oxygen and nutrients, which may not be sufficient for the cells of high respiratory activity. Although the readings may not reflect the real metabolic potential of

HL-60, paradoxically, they are not meaningless, since at some point the OXPHOS phenotype of the cell line is indirectly proven by being the cause of misleading results. Additional confirmation of intensive oxygen consumption comes from high baseline OCR value (**Figure 9A**). Using a lower seeding density could most likely resolve this issue. In fact, in the first trial of the experiment, conducted with even higher seeding density, even more pronounced OCR drop was observed (**Appendix: Figure 23**). The OXPHOS dependency of HL-60 cell line is further reflected by the results obtained in other experiments in this study.

GLUCOSE DEPLETION REDUCED PROLIFERATION IN LEUKEMIA CELL LINES

The importance of glucose availability to maintain highly proliferative phenotype of both leukemia cell lines is confirmed by significant increase in doubling time estimated basing on total 72 h incubation in various glucose growth conditions (**Figure 3, Figure 4, Table 6**). This is in line with widely recognized hallmark of cancer metabolic shift towards glycolysis in order to provide sufficient biosynthetic precursors for abnormal growth and proliferation [47], as well as usage of aerobic glycolysis by normal proliferating cells [63]. In the absence of glucose, leukemia cells switch to alternative metabolic pathways to sustain unaltered viability (**Appendix: Figure 19)**. Glutamine utilization [6, 64, 65], lipolysis [6, 66] or autophagy could constitute possible responses. Role of autophagy in sustaining cell viability was shown in study by Kawaguchi et al. where autophagy inhibition significantly increased Jurkat cell death [67]. Maintenance of energy homeostasis may be attributed to AMPK role in redirecting the metabolism to utilize alternative fuels, as it was shown in study by Chaube et al. where growth of AMPK knocked-down cells in glutamine, lactate and palmitate media was inhibited [68]. Glutamine metabolism, reported to be important in leukemic cells [65], could explain the high pH values observed for NG grown cells, since one of its products is ammonia [69]. Stronger negative impact of glucose depletion on Jurkat cell line proliferative capability reflects their higher dependence on glucose in comparison to HL-60 (**Table 6**). This is in line with previous observation of HL-60 cells having relatively higher OXPHOS capacity [45]. Glucose deprivation may lead to limited proliferation by AMPK activation via increased intracellular AMP/ATP ratio, leading to mTORC1 inhibition and pro-survival [68], rather than pro-proliferative phenotype.

However, to fully unveil the details of the cellular response, further studies need to be employed. All in all, glucose deprivation is a proliferation limiting factor, yet not sufficient to induce cell death in HL-60 or Jurkat. Nevertheless, it could be used as a sensitizing approach for the action of the actual drugs and anti-leukemic agents. In fact, glucose depletion combined with metabolic drug, metformin, shows further inhibition of the proliferation in leukemia cells.

METFORMIN INHIBITS PROLIFERATION REGADRLESS OF METABOLIC PHENOTYPE AND GLUCOSE GROWTH CONDITIONS

The proliferation of both cell lines reduces after the certain threshold of metformin concentration is applied (**Figure 6, Figure 7**). Since metformin manifests its effect by inhibiting Complex I and depolarizing the mitochondrial membrane, certain amount of the drug must be delivered to exert visible influence. The reduction is the most profound when glucose deprived (**Figure 5, Figure 6**), which confirms the role of metabolic stress on the cells becoming more vulnerable to additional stressors. Reduced proliferation when metformin treated in glucose starvation is linked to redirecting the cellular metabolism to maintain the energy homeostasis by other metabolic pathways, which is reflected by somewhat different responses seen in two assays (Figure 5**Figure 6, Figure 7**). Cell cycle arrest, reported in several papers may be the effect of metformin-induced mTOR inhibition, consequently blocking the 4E-BP1 regulator of translation and reducing expression of proteins involved in cell cycle regulation and survival (c-Myc, Cyclin D, Bcl-xL) [28, 70].

GLUCOSE DEPLETION PROMOTES PRO-APOPTOTIC EFFECT OF METFORMIN, ESPECIALLY IN OXPHOS DEPENDENT CELLS

Metformin alone does not affect the viability of leukemia cells, unless applied with glucose depletion (**Figure 21, Figure 22**). The viability decrease is stronger in cells exhibiting more oxidative energy phenotype, which suggests a failure to recover their energy homeostasis once glycolysis and OXPHOS is inhibited. In fact, study by Li et al. showed that HL-60 cells required glycolysis for survival when disrupted the mitochondrial respiratory function [46]. Decrease in MMP and increased ROS levels in glucose starved HL-60 treated with

metformin (**Figure 12A, Figure 14B**) may either further contribute to the cell death or constitute a biomarkers of the cell death ongoing. This is according to studies showing that in some cases MMP loss is a late event in apoptotic process, rather than pro-apoptotic [71]. Pyruvate has been reported as an efficient ROS scavenger, therefore glucose depletion, resulting in reduced formation of pyruvate as the product of glycolysis be partially responsible for increased susceptibility of the cells to oxidative stress [63, 72]. The same molecular mechanisms may explain decrease in Jurkat viability (**Figure 21, Figure 12, Figure 14**). The lesser extent of pro-apoptotic effect in this cell line may be attributed to lower endogenous mitochondrial respiratory capacity (**Figure 9, Figure 11**) [45] and thus, less severe outcome of its inhibition. Moreover, due to loss of PTEN, constantly active PI3K/Akt pathway in this cell line [73] may protect the cells against entering apoptosis via its effectors like p53, FOXO, BAD and NF-κB [29].

GLUCOSE MASKS THE PRO-APOPTOTIC EFFECT OF METFORMIN BY FUELING THE GLYCOLYTIC PATHWAY

In case of both cell lines, glucose abundance masks or reduces the effects of metformin seen in glucose depleted groups (**Appendix: Figure 21, Figure 22**). The drug causes decrease in mitochondrial respiration efficiency in energy production, however, as long as it can be compensated by glycolysis to restore the ATP homeostasis, cells maintain viability, metabolic activity and highly proliferative phenotype, as was observed in this and other studies [74].

ADVERSE METFORMIN EFFECTS IN LEUKEMIA CELL LINES ARE NOT DUE TO ALTERED MITOCHONDRIAL CONTENT

Flowcytometric study showed decrease of MMP in both cell lines upon the treatment (**Figure 12**), which is directly linked to the metformin mode of action, and has been reported in other papers [47]. The slight increase in MMP measured for Jurkat cells treated with metformin in high glucose condition is most likely related to a small induction of mitochondrial biogenesis observed exclusively in this group (**Figure 13**). In fact, metformin stimulated mitochondrial biogenesis was previously reported [75].

REACTIVE OXYGEN SPECIES AND GLUCOSE METABOLISM ARE INTERRELATED IN LEUKEMIA CELLS

Increasing glucose concentration is positively correlated with ROS levels in both cell lines (**Figure 14**), as well as previously indicated proliferation and cell viability. This is in line with a role of high ROS levels to stimulate the pro-survival and pro-proliferative phenotype, which may be attributed to ROS-driven multimodal Akt activation via both inhibition and caseine kinase II mediated degradation of PTEN, as well as direct activation of PI3K [76, 77]. Study by Silva et al. showed that intracellular ROS and PI3K/Akt/mTOR are tightly interconnected, sustain cell viability and regulate glucose uptake [78]. Glucose metabolism and cellular ROS formation have been shown to be positively correlated [79], which is seen in results observed in this study. ROS level decrease in metformin treated HL–60 cells (**Figure 14A**) can be linked to their high mitochondrial respiratory activity, which upon C–I inhibition is highly reduced, and so is the mitochondrial ROS formation. Moreover, pyruvate derived from glycolysis, enhanced to counteract mitochondrial metabolism impairment, may exert an antioxidative effect [63, 72], which is not observed in glucose depleted cells (**Figure 14**).

High glucose grown Jurkat cells responded to metformin treatment by greatly elevated ROS (**Figure 15B**), which can be attributed to glucose redirection towards energy production at the cost of reduced proliferation. These observations may suggest the limited PPP pathway contribution in the stressed glucose metabolism, as the NADPH and ribose-5-phosphate generated by PPP have antioxidative and pro-proliferative roles [79, 80]. Mitochondrial impairment can also contribute to ROS formation [46]. Metformin is the key factor responsible for the ROS enhancement, since once removed, ROS are brought back to levels observed in the control group (**Figure 15B**). This may be attributed to reversibility of C–I inhibition, which diminishes the drug influence on ROS formation, but does not fully restore the proliferative capability of the cells (**Appendix: Table 7, Table 8**). Therefore, metformin treatment leaves anti-proliferative imprint on cellular metabolism.

11. FUTURE PERSPECTIVES AND FINAL REMARKS

SUGGESTIONS ON CURRENT AND FURTHER RESEARCH

The experiments performed in this study were focused on the impact of glucose and metformin on the cells in terms of proliferative capabilities, viability and mitochondrial parameters. This constitutes a solid ground for further investigation of molecular mechanisms involved in the observed effects. It would be of complementary role to determine the expression of the most important metabolic regulators, Akt, AMPK, mTOR. In line with observed viability maintenance, indicating the alternative pathways of energy generation in glucose depleted cells could constitute an additional target for metabolic reprogramming. Introducing glutamine as one more growth condition variable could be an interesting point to start, with its importance for leukemia metabolism indicated in [65, 81]. Supplementary studies on mitochondrial function in two cell lines could give a better understanding of their diverse response to metformin. Agilent Seahorse XFp Cell Mito Stress Test could be one of the options, providing more detailed overview on the mitochondrial respiration than Cell Energy Phenotype Test used in the study. Moreover, individual design of the Mito Stress Test experiment allows to test the direct impact of metformin on the mitochondria and compare it with traditional C-I inhibitor, rotenone [74, 82]. Also, improvement on the Cell Energy Phenotype test for HL-60 cell line could clarify whether the conclusions drawn from our previous experiments were right. In this study, assays used to measure both MMP and mitochondrial biogenesis assessment were based on similar principle, the entry of fluorescent dye into mitochondria driven by MMP. Mitochondrial biogenesis assessment based on different principle, like mtDNA or mitochondrial protein content, could be implemented to re-evaluate the correctness of the previously obtained results [83]. Also, it would be interesting to investigate the effect of long-term metformin treatment of Jurkat cells in HG, as well as in NG grown HL-60, which exhibited significantly decreased viability already after 48h. Evaluation whether PPP, suggested in discussion, is involved in the observed effects could provide further evidence for glucose relevance in dictating the cellular response to metformin.

PHYSIOLOGICAL REALITY AND METFORMIN CONCENTRATION

Metformin has gained a lot of attention as the potential anti-cancer adjuvant drug. The concentration of metformin used in this study was notably higher than achievable in human blood stream, where the actual action site of the drug is if to be applied in anti-leukemic therapy. Therefore, to reinforce the potential of metformin, the first step to be taken should consider the increase of its concentration in the mitochondria of leukemic cells. PolyMetformin, a polymer construct, was shown to exhibit anti-tumor activity exceeding the use of metformin in its natural form in the treatment of melanoma model. PolyMetformin was used in a form of lipid membrane nanoparticle, which allowed additional siRNA incorporation and delivery to the cells, presenting a novel approach for combining metabolic and gene therapy [84]. Similar constructs could be employed in carriage of miRNA, which were shown to be involved to regulate PI3K/Akt/mTOR pathway in many types of leukemia [28]. Another type of polymeric molecules, dendrimers, represent similar approach. Large surface and internal cavities could be used as sites for drug transportation. Moreover, multiple binding sites create an opportunistic solution for molecular targeting [85].

CONCLUSION

Recognition of cancer as a metabolic disease has led the worldwide research to include the metabolic drugs as an integral part of therapeutic strategy to battle cancer. With the universality of metabolic pathways on one hand, and, the diversity of the pathways on the other, approaching cancer appears to be a challenge. Metabolism, the capability of every living creature to maintain the life, constitutes an apparatus for adaptation to the unfavorable conditions, remaining susceptible to their influence at the same time. Diversity of metabolic phenotypes, interrelated to genetic diversity, leads to genuinely broad range of responses to the same stimulus. Cancer represents no exception. Different types of cancers, as well as its distinct cell subpopulations, may in fact represent variety of metabolic phenotypes.

In this study, two leukemia cell lines, shown to possess distinct metabolic profiles, were observed to establish cell line-specific responses to the same external stimuli. Modulation

of glucose growth conditions revealed differential adaptative capabilities, governed by endogenous dependency on glycolytic and oxidative respiration of Jurkat and HL-60, respectively, emphasizing mitochondrial functionality as an important indicator of metabolic flexibility. Susceptibility to the metabolic drug, mitochondrial Complex I inhibitor, was shown to be determined by the phenotype of the cells as well as metabolic reprogramming by glucose availability modulation. Higher endogenous dependency on OXPHOS metabolism was a determinant for greater sensitivity to pro-apoptotic action of metformin, therefore metformin has more potential in the treatment of cancers relying on mitochondrial, rather than glycolytic energy metabolism. This underlines that metabolic phenotyping of cancer prior to the treatment selection is a promising strategy and could significantly contribute to the overall anti-cancer efficiency. However, despite its more pronounced effect in OXPHOS cell line, in general, metformin was shown to have anti-proliferative impact regardless of metabolic preference of the cell line, which supports its choice over other anti-diabetic agents in diabetic population, more susceptible to higher cancer incidence. Based on this and other studies, metformin could be implemented in cancer therapy as an adjuvant drug, sensitizing cancer cells to the actual treatment. In our study we showed that glucose depletion was another crucial determinant of adverse metformin impact. Therefore, agents targeting glucose uptake and metabolism could be a promising complementary treatment. Moreover, it supports the view proposed by other authors that reduced calorie intake and improved glycemia profile in cancer patients could positively affect cancer cells susceptibility. The effect of high glucose concentration masking the metformin action observed in this study points out that evaluation of molecular response to the drug should be performed in lower glucose availability conditions. On the other hand, our finding of oxidative stress in glycolytic cell line indicates that metformin in high glucose condition represent an alternative direction for further investigation, since the mechanism is still to be unveiled. Majority of our findings are dictated by short-term of metformin exposure. Nevertheless, our data suggests that to maintain the beneficial therapeutic effect, the drug concentration should be kept at the same level by regular supplementation.

12. REFERENCES

[1] Wishart, D.S. Is Cancer a Genetic Disease or a Metabolic Disease? *EBioMedicine*, **2015**, *2,* 478–479.

[2] Hannah Ritchie and Max Roser. Causes of Death. https://ourworldindata.org/causes-of-death (Accessed May 22, 2018).

[3] Seyfried, T.N.; Flores, R.E.; Poff, A.M.; D'Agostino, D.P. Cancer as a metabolic disease: Implications for novel therapeutics. *Carcinogenesis*, **2014**, *35,* 515–527.

[4] Seyfried, T.N.; Shelton, L.M. Cancer as a metabolic disease. *Nutrition & metabolism*, **2010**, *7,* 7.

[5] Courtnay, R.; Ngo, D.C.; Malik, N.; Ververis, K.; Tortorella, S.M.; Karagiannis, T.C. Cancer metabolism and the Warburg effect: The role of HIF-1 and PI3K. *Molecular biology reports*, **2015**, *42,* 841–851.

[6] Seyfried, T.N. *Cancer as a metabolic disease: On the origin, management, and prevention of cancer;* Wiley: Hoboken N.J., **2012**.

[7] Zheng, J. Energy metabolism of cancer: Glycolysis versus oxidative phosphorylation (Review). *Oncology letters*, **2012**, *4,* 1151–1157.

[8] Fu, Y.; Liu, S.; Yin, S.; Niu, W.; Xiong, W.; Tan, M.; Li, G.; Zhou, M. The reverse Warburg effect is likely to be an Achilles' heel of cancer that can be exploited for cancer therapy. *Oncotarget*, **2017**, *8,* 57813–57825.

[9] Gonzalez, C.D.; Alvarez, S.; Ropolo, A.; Rosenzvit, C.; Bagnes, M.F.G.; Vaccaro, M.I. Autophagy, Warburg, and Warburg reverse effects in human cancer. *BioMed research international*, **2014**, *2014,* 926729.

[10] Tidwell, T.R.; Søreide, K.; Hagland, H.R. Aging, Metabolism, and Cancer Development: From Peto's Paradox to the Warburg Effect. *Aging and disease*, **2017**, *8,* 662–676.

[11] Hagland, H.R.; Søreide, K. Cellular metabolism in colorectal carcinogenesis: Influence of lifestyle, gut microbiome and metabolic pathways. *Cancer letters*, **2015**, *356,* 273–280.

[12] Hanahan, D.; Weinberg, R.A. The Hallmarks of Cancer. *Cell*, **2000**, *100,* 57–70.

[13] Vander Heiden, M.G.; Cantley, L.C.; Thompson, C.B. Understanding the Warburg effect: The metabolic requirements of cell proliferation. *Science (New York, N.Y.)*, **2009**, *324,* 1029–1033.

[14] Owens, K.M.; Modica-Napolitano, J.S.; Singh, K.K. *Mitochondria and Cancer*.

[15] Ngo, D.C.; Ververis, K.; Tortorella, S.M.; Karagiannis, T.C. Introduction to the molecular basis of cancer metabolism and the Warburg effect. *Molecular biology reports*, **2015**, *42,* 819–823.

[16] Lemarie, A.; Grimm, S. Mitochondrial respiratory chain complexes: Apoptosis sensors mutated in cancer? *Oncogene*, **2011**, *30,* 3985–4003.

[17] Lodish. *Molecular Cell Biology*.

[18] Archibald, J.M. Endosymbiosis and Eukaryotic Cell Evolution. *Current biology : CB*, **2015**, *25,* R911-21.

[19] Srivastava, N.; Pande, M. Mitochondrion: Features, functions and comparative analysis of specific probes in detecting sperm cell damages. *Asian Pacific Journal of Reproduction*, **2016**, *5,* 445–452.

[20] Liza A. Pon, Eric A. Schon. *Mitochondria,* 2nd ed.; Elsevier, **2007**.

[21] Schieber, M.; Chandel, N.S. ROS function in redox signaling and oxidative stress. *Current biology : CB*, **2014**, *24,* R453-62.

[22] Wallace, D.C. Mitochondria and cancer. *Nature reviews. Cancer*, **2012**, *12,* 685–698.

[23] Murphy, M.P. How mitochondria produce reactive oxygen species. *The Biochemical journal*, **2009**, *417,* 1–13.

[24] Salk, J.J.; Fox, E.J.; Loeb, L.A. Mutational heterogeneity in human cancers: Origin and consequences. *Annual review of pathology*, **2010**, *5,* 51–75.

[25] Rathmell, J.C.; Fox, C.J.; Plas, D.R.; Hammerman, P.S.; Cinalli, R.M.; Thompson, C.B. Akt-Directed Glucose Metabolism Can Prevent Bax Conformation Change and Promote Growth Factor-Independent Survival. *Molecular and Cellular Biology*, **2003**, *23,* 7315–7328.

[26] Xilan Yu, Wuxiang Mao, Yansheng Zhai, Chong Tong, Min Liu, Lixin Ma, Xiaolan Yu, Shanshan Li. Anti-tumor activity of metformin: from metabolic and epigenetic perspectives. *Oncotarget*, **2017**, *8,* 5619–5628.

[27] Herschbein, L.; Liesveld, J.L. Dueling for dual inhibition: Means to enhance effectiveness of PI3K/Akt/mTOR inhibitors in AML. *Blood reviews*, **2018**, *32,* 235–248.

[28] Bertacchini, J.; Heidari, N.; Mediani, L.; Capitani, S.; Shahjahani, M.; Ahmadzadeh, A.; Saki, N. Targeting PI3K/AKT/mTOR network for treatment of leukemia. *Cellular and molecular life sciences : CMLS*, **2015**, *72,* 2337–2347.

[29] Chalhoub, N.; Baker, S.J. PTEN and the PI3-kinase pathway in cancer. *Annual review of pathology*, **2009**, *4,* 127–150.

[30] Giancotti, F.G. Deregulation of cell signaling in cancer. *FEBS letters*, **2014**, *588,* 2558–2570.

[31] Sośnicki, S.; Kapral, M.; Węglarz, L. Molecular targets of metformin antitumor action. *Pharmacological reports : PR*, **2016**, *68,* 918–925.

[32] Griss, T.; Vincent, E.E.; Egnatchik, R.; Chen, J.; Ma, E.H.; Faubert, B.; Viollet, B.; DeBerardinis, R.J.; Jones, R.G. Metformin Antagonizes Cancer Cell Proliferation by Suppressing Mitochondrial-Dependent Biosynthesis. *PLoS biology*, **2015**, *13,* e1002309.

[33] GG Graham JPunt MArora RO Day MP Doogue JK Duong TJ Furlong JR Greenfield LC Greenup CM Kirkpatrick JE Ray PTimmins KM Williams. Clinical Pharmacokinetics 2011;

[34] Ferrannini, E. The target of metformin in type 2 diabetes. *The New England journal of medicine*, **2014**, *371,* 1547–1548.

[35] Andrzejewski, S.; Gravel, S.-P.; Pollak, M.; St-Pierre, J. Metformin directly acts on mitochondria to alter cellular bioenergetics. *Cancer & metabolism*, **2014**, *2,* 12.

[36] Vallianou, N.G.; Evangelopoulos, A.; Kazazis, C. Metformin and cancer. *The review of diabetic studies : RDS*, **2013**, *10,* 228–235.

[37] Mallik, R.; Chowdhury, T.A. Metformin in cancer. *Diabetes research and clinical practice*, **2018**.

[38] Castillo-Quan, J.I.; Blackwell, T.K. Metformin: Restraining Nucleocytoplasmic Shuttling to Fight Cancer and Aging. *Cell*, **2016**, *167,* 1670–1671.

[39] Pietrocola F., K.G. Metformin: a metabolic modulator. *Oncotarget*, **2017**, *8,* 9017–9020.

[40] Bozzone, D. *The biology of Cancer: Leukemia;* Chelsea House: USA, **2009**.

[41] Kampen, K.R. The discovery and early understanding of leukemia. *Leukemia research*, **2012**, *36,* 6–13.

[42] Mughal, T.I.; Goldman, J.M.; Mughal, S.T. *Understanding leukemias, lymphomas, and myelomas;* Taylor & Francis: London, New York, **2006**.

[43] Deynoux, M.; Sunter, N.; Hérault, O.; Mazurier, F. Hypoxia and Hypoxia-Inducible Factors in Leukemias. *Frontiers in oncology*, **2016**, *6,* 41.

[44] Aghvami, M.; Ebrahimi, F.; Zarei, M.H.; Salimi, A.; Pourahmad Jaktaji, R.; Pourahmad, J. Matrine Induction of ROS Mediated Apoptosis in Human ALL B-lymphocytes Via Mitochondrial Targeting. *Asian Pacific journal of cancer prevention : APJCP*, **2018**, *19,* 555–560.

[45] Coombs, C.C.; Tavakkoli, M.; Tallman, M.S. Acute promyelocytic leukemia: Where did we start, where are we now, and the future. *Blood cancer journal*, **2015**, *5,* e304.

[46] Rashidi, A.; Fisher, S.I. Therapy-related acute promyelocytic leukemia: A systematic review. *Medical oncology (Northwood, London, England)*, **2013**, *30,* 625.

[47] Ng, C.-H.; Chng, W.-J. Recent advances in acute promyelocytic leukaemia. *F1000Research*, **2017**, *6,* 1273.

[48] Elbahesh E., Patel N., Tabbara I.A. Treatment of Acute Promyelocytic Leukemia. *Anticancer Research*, **2014**, *34,* 1507–1518.

[49] Fantin, V.R.; Leder, P. Mitochondriotoxic compounds for cancer therapy. *Oncogene*, **2006**, *25,* 4787–4797.

[50] Osellame, L.D.; Blacker, T.S.; Duchen, M.R. Cellular and molecular mechanisms of mitochondrial function. *Best practice & research. Clinical endocrinology & metabolism*, **2012**, *26,* 711–723.

[51] John R.W. Masters, Bernerd O. Palsson. *Human Cell Cutlure: Part 3: Leukemias and Lymphomas;* Kluwer Avademic Publishers: New York, **2000**.

[52] Erikstein, B.S.; Hagland, H.R.; Nikolaisen, J.; Kulawiec, M.; Singh, K.K.; Gjertsen, B.T.; Tronstad, K.J. Cellular stress induced by resazurin leads to autophagy and cell death via production of reactive oxygen species and mitochondrial impairment. *Journal of cellular biochemistry*, **2010**, *111,* 574–584.

[53] Li, N.; Oquendo, E.; Capaldi, R.A.; Robinson, J.P.; He, Y.D.; Hamadeh, H.K.; Afshari, C.A.; Lightfoot-Dunn, R.; Narayanan, P.K. A systematic assessment of mitochondrial function identified novel signatures for drug-induced mitochondrial disruption in cells. *Toxicological sciences : an official journal of the Society of Toxicology*, **2014**, *142,* 261–273.

[54] Scotland, S.; Saland, E.; Skuli, N.; Toni, F. de; Boutzen, H.; Micklow, E.; Sénégas, I.; Peyraud, R.; Peyriga, L.; Théodoro, F.; Dumon, E.; Martineau, Y.; Danet-Desnoyers, G.; Bono, F.; Rocher, C.; Levade, T.; Manenti, S.; Junot, C.; Portais, J.-C.; Alet, N.; Récher, C.; Selak, M.A.; Carroll, M.; Sarry, J.-E. Mitochondrial energetic and AKT status mediate metabolic effects and apoptosis of metformin in human leukemic cells. *Leukemia*, **2013**, *27,* 2129–2138.

[55] Rodríguez-Lirio, A.; Pérez-Yarza, G.; Fernández-Suárez, M.R.; Alonso-Tejerina, E.; Boyano, M.D.; Asumendi, A. Metformin Induces Cell Cycle Arrest and Apoptosis in Drug-Resistant Leukemia Cells. *Leukemia research and treatment*, **2015**, *2015,* 516460.

[56] Merck Millipore. MCH100102 Muse Count&Viability Assay Kit. http://www.merckmillipore.com/NO/en/product/Muse-Count-ampViability-Assay-Kit-100-Tests,MM_NF-MCH100102?CatalogCategoryID=# (Accessed June 6, 2018).

[57] Merck Millipore. MuseSoft. http://www.merckmillipore.com/NO/en/life-science-research/cell-analysis-flow-cytometry/muse-cell-analyzer/instrument-registration-software-updates/QkOb.qB.LQUAAAFB1r4WFVt3,nav (Accessed June 6, 2018).

[58] Millipore Corporation. BrdU Cell Proliferation Assay: Cat. No. 2750. http://www.merckmillipore.com/NO/en/product/BrdU-Cell-Proliferation-Kit,MM_NF-2750 (Accessed June 6, 2018).

[59] Agilent Technologies. How to Hydrate an Agilent Seahorse XFp Sensor Cartridge: For use with the Agilent Seahorse XFp Analyzer. https://www.agilent.com/cs/library/usermanuals/public/Hydrating_an_XFp_Sensor_Cartridge.pdf (Accessed June 2, 2018).

[60] Agilent Technologies. Preparation of XFp assay media. https://www.agilent.com/cs/library/usermanuals/public/Media%20Prep%20XFp.pdf (Accessed June 2, 2018).

[61] Corning Incorporated. Corning Cell-Tak Cell and Tissue Adhesive: Instructions for use. https://www.corning.com/catalog/cls/documents/product-information-sheets/SPC-354240.pdf (Accessed June 2, 2018).

[62] Agilent Technologies. Immobilization of Non-Adherent Cells with Cell-Tak for Assay on the Agilent Seahorse XFe/XF96 or XFp Analyzer. https://www.agilent.com/cs/library/technicaloverviews/public/5991-7153EN.pdf (Accessed June 2, 2018).

[63] Agilent Technologies. Agilent Seahorse XFp Cell Energy Phenotype Test Kit. https://www.agilent.com/cs/library/usermanuals/public/XFp_Cell_Energy_Phenotype_Test_Kit_User_Guide.pdf (Accessed June 2, 2018).

[64] Agilent Technologies. Agilent Seahorse Wave Desktop software. https://www.agilent.com/en/products/cell-analysis/software-download-for-wave-desktop (Accessed June 6, 2018).

[65] Invitrogen™ Tetramethylrhodamine, Methyl Ester, Perchlorate (TMRM): Catalog number: T668. https://www.thermofisher.com/order/catalog/product/T668.

[66] Thermo Fisher. Invitrogen™ MitoTracker™ Deep Red FM: Catalog number: M22426. https://www.thermofisher.com/order/catalog/product/M22426 (Accessed June 6, 2018).

[67] Invitrogen™ CM-H2DCFDA (General Oxidative Stress Indicator): Catalog number: C6827. https://www.thermofisher.com/order/catalog/product/C6827 (Accessed June 6, 2018).

[68] Karl A. Brand, Ulrich Hermfisse. Aerobic glycolysis by proliferating cells: a protective strategy against reactive oxygen species. *FABEB J.*, **1997**, *11,* 388–395.

[69] Polet, F.; Martherus, R.; Corbet, C.; Pinto, A.; Feron, O. Inhibition of glucose metabolism prevents glycosylation of the glutamine transporter ASCT2 and promotes compensatory LAT1 upregulation in leukemia cells. *Oncotarget*, **2016**, *7,* 46371–46383.

[70] Baumann, S. Starvation of Jurkat T cells causes metabolic switch from glycolysis to lipolysis as revealed by comprehensive GC-qMS. *JIOMICS*, **2013**, *3*.

[71] Kawaguchi, M.; Aoki, S.; Hirao, T.; Morita, M.; Ito, K. Autophagy is an important metabolic pathway to determine leukemia cell survival following suppression of the

glycolytic pathway. *Biochemical and biophysical research communications*, **2016**, *474,* 188–192.

[72] Chaube, B.; Malvi, P.; Singh, S.V.; Mohammad, N.; Viollet, B.; Bhat, M.K. AMPK maintains energy homeostasis and survival in cancer cells via regulating p38/PGC-1α-mediated mitochondrial biogenesis. *Cell death discovery*, **2015**, *1,* 15063.

[73] Elisa Vega Avila, Michael K. Pugsley. Colorimetric assays used to measure survival or proliferation of cells: a review. *Proc. West. Pharmacol. Soc.*, **2011**, *54,* 10–14.

[74] Zhang, B.; Liu, L.-L.; Mao, X.; Zhang, D.-H. Effects of metformin on FOXM1 expression and on the biological behavior of acute leukemia cell lines. *Molecular medicine reports*, **2014**, *10,* 3193–3198.

[75] Ly, J.D.; Grubb, D.R.; Lawen, A. The mitochondrial membrane potential (Δψm) in apoptosis; an update. *APOPTOSIS*, **2003**, *8,* 115–128.

[76] Daniel Kuc. Pyruvate is an endogenous anti-inflammatory and anti-oxidant molecule. *Med Sci Monit*, **2006**, *12,* 79–84.

[77] Freeley, M.; Park, J.; Yang, K.-J.; Wange, R.L.; Volkov, Y.; Kelleher, D.; Long, A. Loss of PTEN expression does not contribute to PDK-1 activity and PKC activation-loop phosphorylation in Jurkat leukaemic T cells. *Cellular signalling*, **2007**, *19,* 2444–2457.

[78] William W. Wheaton et al. Metformin inhibits mitochondrial complex I of cancer cells to reduce tumorigenesis. *eLife*, **2014**, *3*.

[79] Loubiere, C.; Clavel, S.; Gilleron, J.; Harisseh, R.; Fauconnier, J.; Ben-Sahra, I.; Kaminski, L.; Laurent, K.; Herkenne, S.; Lacas-Gervais, S.; Ambrosetti, D.; Alcor, D.; Rocchi, S.; Cormont, M.; Michiels, J.-F.; Mari, B.; Mazure, N.M.; Scorrano, L.; Lacampagne, A.; Gharib, A.; Tanti, J.-F.; Bost, F. The energy disruptor metformin targets mitochondrial integrity via modification of calcium flux in cancer cells. *Scientific reports*, **2017**, *7,* 5040.

[80] Silva, A.; Yunes, J.A.; Cardoso, B.A.; Martins, L.R.; Jotta, P.Y.; Abecasis, M.; Nowill, A.E.; Leslie, N.R.; Cardoso, A.A.; Barata, J.T. PTEN posttranslational inactivation and hyperactivation of the PI3K/Akt pathway sustain primary T cell leukemia viability. *The Journal of clinical investigation*, **2008**, *118,* 3762–3774.

[81] Zhang, J.; Wang, X.; Vikash, V.; Ye, Q.; Wu, D.; Liu, Y.; Dong, W. ROS and ROS-Mediated Cellular Signaling. *Oxidative medicine and cellular longevity*, **2016**, *2016,* 4350965.

[82] Silva, A.; Gírio, A.; Cebola, I.; Santos, C.I.; Antunes, F.; Barata, J.T. Intracellular reactive oxygen species are essential for PI3K/Akt/mTOR-dependent IL-7-mediated viability of T-cell acute lymphoblastic leukemia cells. *Leukemia*, **2011**, *25,* 960–967.

[83] Liemburg-Apers, D.C.; Willems, P.H.G.M.; Koopman, W.J.H.; Grefte, S. Interactions between mitochondrial reactive oxygen species and cellular glucose metabolism. *Archives of toxicology*, **2015**, *89,* 1209–1226.

[84] Kang, S.W.; Lee, S.; Lee, E.K. ROS and energy metabolism in cancer cells: Alliance for fast growth. *Archives of pharmacal research*, **2015**, *38,* 338–345.

[85] Wise, D.R.; Thompson, C.B. Glutamine addiction: A new therapeutic target in cancer. *Trends in biochemical sciences*, **2010**, *35,* 427–433.

[86] Polet, F.; Martherus, R.; Corbet, C.; Pinto, A.; Feron, O. Inhibition of glucose metabolism prevents glycosylation of the glutamine transporter ASCT2 and promotes compensatory LAT1 upregulation in leukemia cells. *Oncotarget*, **2016**, *7,* 46371–46383.

[87] Zhao, Y.; Wang, W.; Guo, S.; Wang, Y.; Miao, L.; Xiong, Y.; Huang, L. PolyMetformin combines carrier and anticancer activities for in vivo siRNA delivery. *Nature communications*, **2016**, *7,* 11822.

[88] Mendivil-Perez, M.; Jimenez-Del-Rio, M.; Velez-Pardo, C. Response to rotenone is glucose-sensitive in a model of human acute lymphoblastic leukemia: Involvement of oxidative stress mechanism, DJ-1, Parkin, and PINK-1 proteins. *Oxidative medicine and cellular longevity*, **2014**, *2014,* 457154.

[89] Perry, S.W.; Norman, J.P.; Barbieri, J.; Brown, E.B.; Gelbard, H.A. Mitochondrial membrane potential probes and the proton gradient: A practical usage guide. *BioTechniques*, **2011**, *50,* 98–115.

[90] Wu, L.-P.; Ficker, M.; Christensen, J.B.; Trohopoulos, P.N.; Moghimi, S.M. Dendrimers in Medicine: Therapeutic Concepts and Pharmaceutical Challenges. *Bioconjugate chemistry*, **2015**, *26,* 1198–1211.

13. APPENDIX

PROLIFERATION ASSAY IN DIFFERENT GLUCOSE GROWTH CONDITIONS

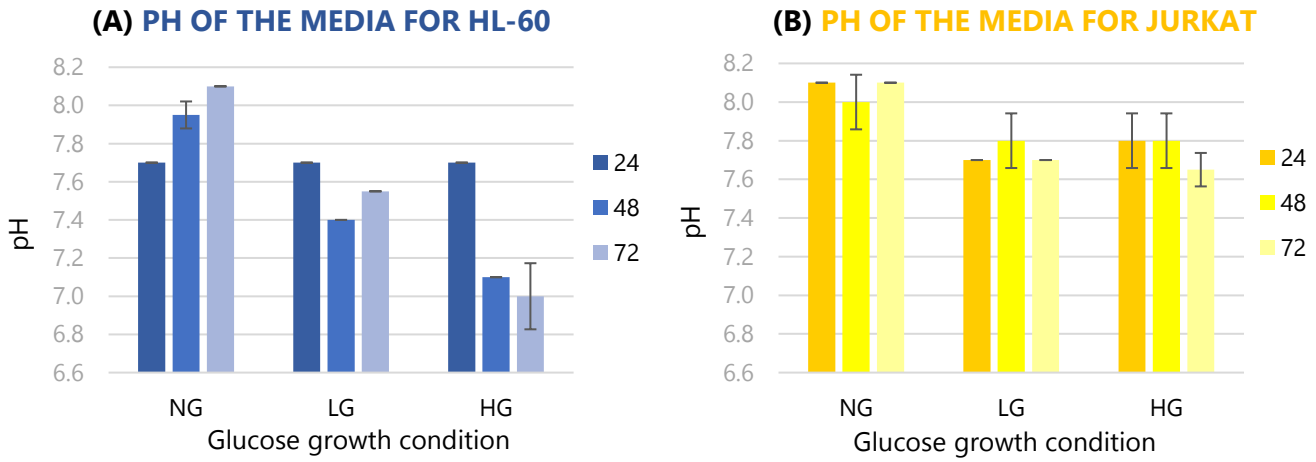

Figure 18 Proliferation assay with glucose: pH of the media. HL-60 (A) and Jurkat (B) cells were grown for 24h, 48h and 72h in different glucose growth conditions: NG, LG and HG. Numbers based on pH measurement with test stripes. N=3.

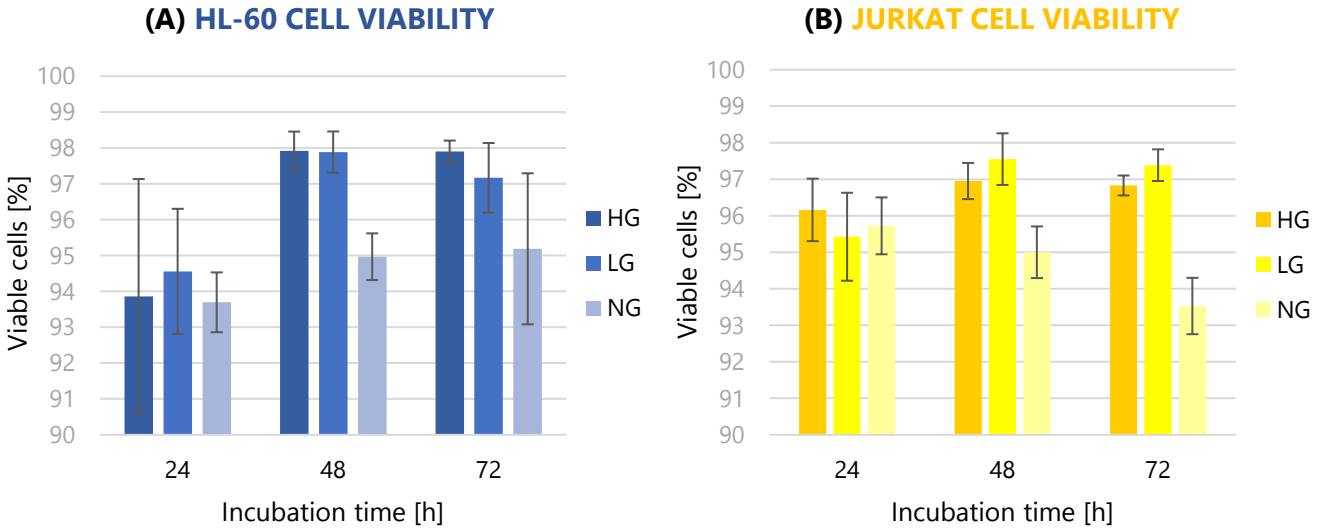

Figure 19 Proliferation assay with glucose. Cell viability. HL-60 (A) and Jurkat (B) cell viability grown in HG, LG and NG conditions for 24h, 48h and 72h. Numbers based on the results obtained in MUSE Count&Viability Assay. N=3.

PROLIFERATION ASSAY IN DIFFERENT GLUCOSE GROWTH CONDITIONS WITH METFORMIN TREATMENT FOR 48H

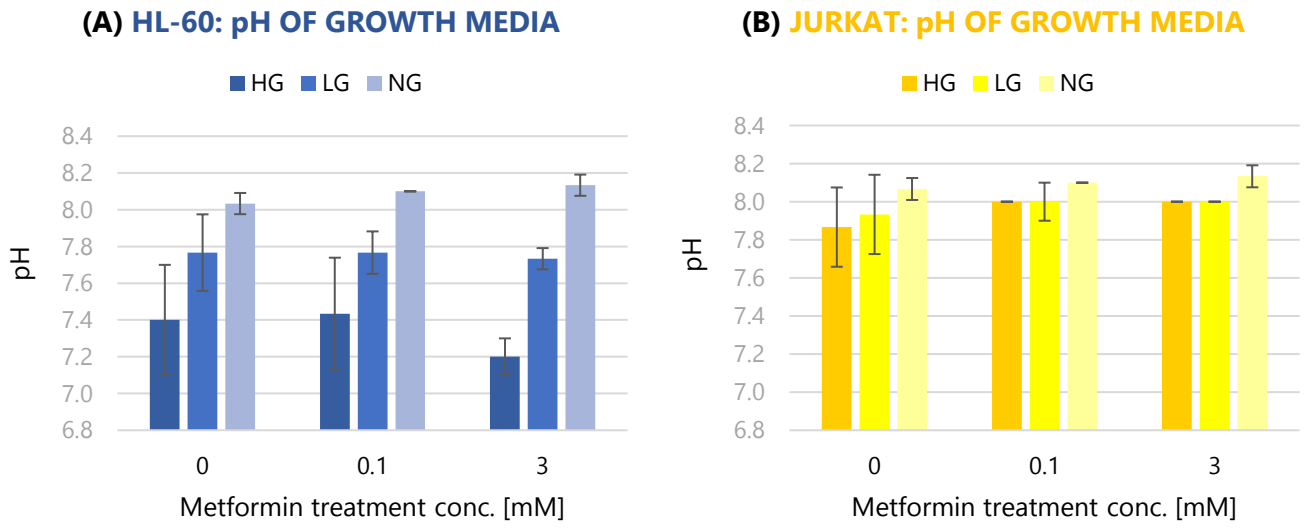

Figure 20 Proliferation assay with metformin. pH of the media. pH values measured after 48h of incubation of HL-60 (A) and Jurkat cells (B) with 0.0 mM, 0.1 mM and 3.0 mM metformin treatment in different glucose growth conditions. Starting pH of the media had been measured to be 7.9, 8.0 and 8.1 for HG, LG and NG, respectively. Numbers based on measurements with test stripes. N=3.

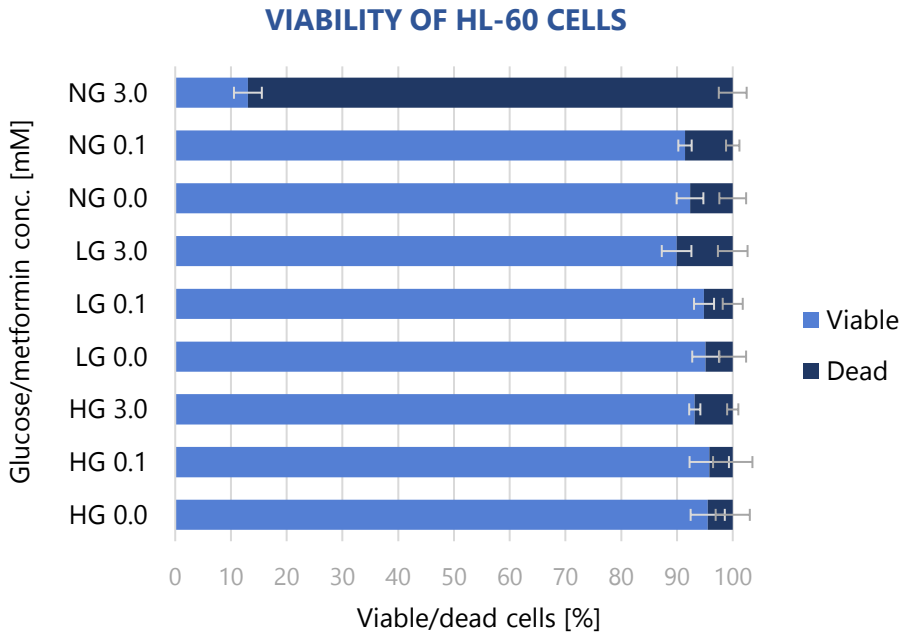

Figure 21 Proliferation assay with metformin: HL-60 cell viability. Numbers after 48h growth in different glucose conditions and metformin treatment of 0.0 mM, 0.1 mM and 3.0 mM. Data obtained by MUSE Count&Viability Assay. N=3.

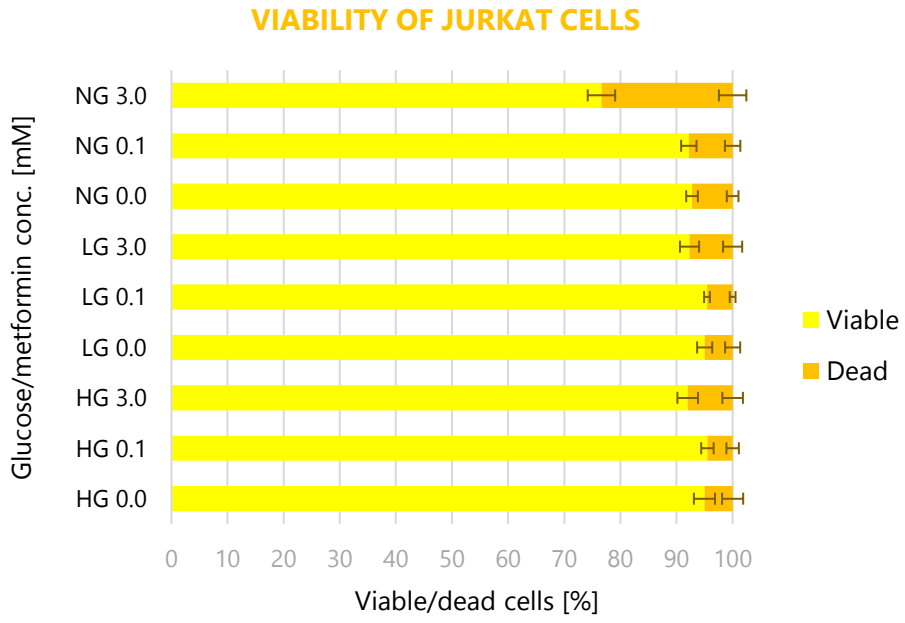

Figure 22 Proliferation assay with metformin: Jurkat cell viability. Numbers after 48h growth in different glucose conditions and metformin treatment of 0.0 mM, 0.1 mM and 3.0 mM. Data obtained by MUSE Count&Viability Assay. N=3.

FLOW CYTOMETRIC STUDY ON METFORMIN REMOVAL EFFECT IN JURKAT CELLS

Table 7 Count&Viability Assay results for Jurkat cells grown for 48h in HG 0.0 mM Met and 3.0 mM Met conditions. Data obtained by MUSE Count&Viability Assay. pH of the media values based on test stripes measurements.

Sample		Viable cells conc. [cells/ml]	pH	Population profile	
				Viable	Dead
0.0 mM Met	BR 1	1480000	7.4	96.4%	3.6%
	BR 2	1550000	7.4	97.1%	2.9%
	BR 3	1440000	7.7	95.8%	4.2%
3.0 mM Met	BR 1	892000	7.1	95.8%	4.2%
	BR 2	866000	7.4	96.0%	4.0%
	BR 3	918000	7.4	96.8%	3.2%

Table 8 Count&Viability results for Jurkat cells grown for 96h in differential conditions: 48h in HG 0.0 mM Met + 48h in HG 0.0 mM Met or 48h in HG 3.0 mM Met + 48h 0.0 mM Met. Data obtained by MUSE Count&Viability Assay. pH of the media values based on test stripes measurements.

Sample		Viable cells conc. [cells/ml]	pH	Population profile	
				Viable	Dead
0.0 mM Met + 0.0 mM Met	BR 1	1520000	7.4	96.2%	3.8%
	BR 2	1560000	7.4	97.9%	2.1%
	BR 3	1570000	7.4	96.6%	3.4%
3.0 mM Met + 0.0 mM Met	BR 1	1160000	7.7	95.0%	5.0%
	BR 2	940000	7.7	96.3%	3.7%
	BR 3	1420000	7.7	96.7%	3.3%

ENERGY PHENOTYPE TEST

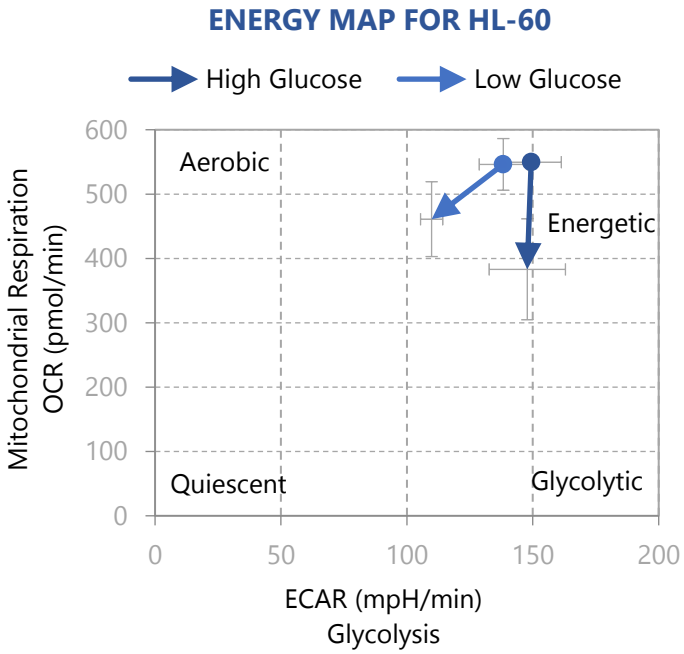

Figure 23 Cell Energy Phenotype Test. Energy Map for HL-60 cells seeded in density of 100 000 cells/well.

TABLES WITH MATERIALS USED IN THE PROJECT

Table 9 List of reagents used in the project

NAME	CATALOG No.	COMPANY
RPMI 1640 1X medium with L-glutamine	10-040-CVR	Corning, Mediatech, Inc., USA
RPMI 1640 1X medium with L-glutamine without glucose	10-043-CVR	Corning, Mediatech, Inc., USA
FBS Heat Inactivated, South America Origin	S181H-500	Biovest, France
Penilicillin-Streptomycin	L0018-100	Biovest, France
Metformin hydrochoride	PHR 1084-500mg	Sigma Aldrich, USA

Tryphan Blue 0.4%	K940-100ML	Nalgene, Amresco, Ohio
DMSO	A3672, 0100	AppliChem, Panreac, Germany
L-glutamine	25-005-CI	Corning, USA
Seahorse XF Base Medium, (DMEM), 500 mL	103334-100	Agilent Technologies
Seahorse XF Calibrant Solution 100 mL	103059-000	Agilent Technologies
Seahorse XFp Cell Culture Miniplate	103025-100	Agilent Technologies
Seahorse XFp FluxPak: Sensor Cartridges with utility Miniplates for calibration	103022-100	Agilent Technologies
Sodium pyruvate		Sigma Aldrich, USA
Seahorse XFp Cell Energy Phenotype Test Kit	103275-100	Agilent Technologies
D-(+)-Glucose	G8270	Sigma Aldrich, USA
CM-H2DCFDA (General Oxidative Stress Indicator)	C6827	Invitrogen, Thermo Fisher Scientific, USA
MitoTracker™ Deep Red FM	M22426	Invitrogen, Thermo Fisher Scientific, USA
Tetramethylrhodamine, Methyl Ester, Perchlorate (TMRM)	T668	Invitrogen, Thermo Fisher Scientific, USA
MColorpHast™ non-bleeding pH-indicator strips pH 6.5 – 10.0	109543	Merck KGaA, Germany
Phosphate buffered saline	P4417	Sigma Aldrich, USA
6-well plates, flat bottom, TC-treated	734-2323	VWR, UK
12-well plates, flat bottom, TC-treated	734-2324	VWR, UK

96-well Black/Clear Flat Bottom TC treated plate	353219	Falcon®, Corning, USA
Tissue Culture Flask, 50 mL, 25cm^2	353108	Falcon®, Corning, USA
Tissue Culture Flask, 250 mL, 75cm^2	353135	Falcon®, Corning, USA
Tissue Culture Flask, 250 mL, 75cm^2	353136	Falcon®, Corning, USA
Tissue Culture Flask, 250 mL, 75cm^2	658170	CellStar®, Greiner bio-one
alamarBlue® Cell Viability Assay	786-922	G Biosciences, USA
alamarBlue® Cell Viabilty Assay	DAL1025	Thermo Fisher Scientific, USA
BrdU Cell Proliferation Assay	2752	Millipore Corporation/ Merck, KGaA, Germany
Muse® Count & Viability Assay Kit	MCH600103	EMD Millipore Corporation, USA

Table 10 List of instruments used in the project

NAME	CATALOG No.	COMPANY
INCU-Line® IL 10 Digital incubator	390-0384	VWR
SpectraMax® Paradigm® Multi-Mode Detection Platform	Part nr: Paradigm Device serial nr: 33270-1108	Molecular Devices
Seahorse XFp Analyzer	Part nr: 102745-100 Serial nr: US430356	Agilent Technologies
Agilent Seahorse Wave Desktop Software	Version 2.4.0.60	Agilent Technologies
Muse® Cell Analyzer		EMD Millipore Corporation/Merck KgaA, Germany

Muse® Software	Version 1.5.0.0	EMD Millipore Corporation/Merck KgaA, Germany
Heated circulating bath Type T100-ST12/18	Ser no: T01734023	Grant Instruments (Cambridge) Ltd
Labgard Class II Laminar Flow Biological Safety Cabinet NU-436-400E	Ser no: 111225120606	NuAire, Inc., USA
Class II Biological Safety Cabinet MSC-Advantage™ 1.2	Ser no: 41085135	Thermo Fisher Scientific Inc., USA
CO_2 Incubator MCO-18AIC(UV)	Ser no: 60711645	SANYO Electric Co., Lts., Japan
CO_2 Incubator NU-5510E	Ser no: 123651060208	NuAire, Inc., USA
Accuri C6 Flow cytometer		BD Biosciences, USA
CFlow®	Version 1.0.227.4	Accuri ® Cytometers, Inc.